ISSN : 2165-4069(Online)
ISSN : 2165-4050(Print)

IJARAI

International Journal of Advanced Research in Artificial Intelligence

Volume 5 Issue 12

www.ijarai.thesai.org

A Publication of
The Science and Information Organization

Editorial Preface

From the Desk of Managing Editor…

Artificial Intelligence is hardly a new idea. Human likenesses, with the ability to act as human, dates back to Geek mythology with Pygmalion's ivory statue or the bronze robot of Hephaestus. However, with innovations in the technological world, AI is undergoing a renaissance that is giving way to new channels of creativity.

The study and pursuit of creating artificial intelligence is more than designing a system that can beat grand masters at chess or win endless rounds of Jeopardy!. Instead, the journey of discovery has more real-life applications than could be expected. While it may seem like it is out of a science fiction novel, work in the field of AI can be used to perfect face recognition software or be used to design a fully functioning neural network.

At the International Journal of Advanced Research in Artificial Intelligence, we strive to disseminate proposals for new ways of looking at problems related to AI. This includes being able to provide demonstrations of effectiveness in this field. We also look for papers that have real-life applications complete with descriptions of scenarios, solutions, and in-depth evaluations of the techniques being utilized.

Our mission is to be one of the most respected publications in the field and engage in the ubiquitous spread of knowledge with effectiveness to a wide audience. It is why all of articles are open access and available view at any time.

IJARAI strives to include articles of both research and innovative applications of AI from all over the world. It is our goal to bring together researchers, professors, and students to share ideas, problems, and solution relating to artificial intelligence and application with its convergence strategies. We would like to express our gratitude to all authors, whose research results have been published in our journal, as well as our referees for their in-depth evaluations.

We hope that this journal will inspire and educate. For those who may be enticed to submit papers, thank you for sharing your wisdom.

Editor-in-Chief
IJARAI
Volume 5 Issue 12 December 2016
ISSN: 2165-4069(Online)
ISSN: 2165-4050(Print)

Editorial Board

Reviewer Board Members

CONTENTS

Paper 1: Size Distribution Estimation Method using Reflected Laser Light Angle Dependency by Rain Droplets
Authors: Kohei Arai
PAGE 1 – 7

Paper 2: Data Hiding Method Replacing LSB of Hidden Portion for Secret Image with Run-Length Coded Image
Authors: Kohei Arai
PAGE 8 – 14

Paper 3: Development of Decision Support System to Selection of the Blended Learning Platforms for Mathematics and ICT Learning at SMK TI Udayana
Authors: I Made Ardana, I Putu Wisna Ariawan, Dewa Gede Hendra Divayana
PAGE 15 – 18

Paper 4: Neural Backpropagation System for the Study of Obesity in Childhood
Authors: A. Medina-Santiago, E. M. Melgar-Paniagua, L. C. Campos-Reyes, A. Cisneros-Gómez, N. R. García-Chong
PAGE 19 – 23

Size Distribution Estimation Method using Reflected Laser Light Angle Dependency by Rain Droplets

Kohei Arai[1]
[1]Graduate School of Science and Engineering
Saga University
Saga City, Japan

***Abstract*—Methods for size distribution estimation and rainfall type discrimination with estimated phase function using measured reflected laser light by rain droplet are proposed. Preliminary experiments are conducted with Laser ranging instrument and spectral radiometer for estimation of size distribution and rainfall type discrimination as well as phase function of scattering by rain drops. Through the experiments, it is found that rainfall type can be discriminated together with rain droplet size distribution estimation.**

Keywords—Rainfall; Laser ranging; Marshall Palmer distribution; Rayleigh scattering; Mie scattering; Phase function; Rain drpolet size distribution

I. INTRODUCTION

Land slide detection and prediction due to heavy rain is important. Therefore, not so small number of systems are proposed so far. It requires quit high sensitivity of a tiny slide (mm order) has to be detected for prediction. The proposed method ensures that such high sensitivity of a slide in the order of mm. Landslide is one of severe disaster. In order to monitor landslides, several methods have been proposed so far. One of the conventional land slide monitoring systems is to measure the resistance of the wire which is set at potential landslide steeply slopes. Although it is simple and cheap system, measurement accuracy is not so good in terms of the distance between two ends of the wire which depends on resistance. Therefore, it cannot be used for making caution for evacuation from the potential landslide area. Other wide variety of commercial off-the-shelf electronic and/or mechanical geotechnical and hydrologic sensors exist [1],[2]. Meanwhile, satellite remote sensing imagery data is used for disaster relief due to landslide. It cannot be used for landslide warning system. There are so many previously proposed methods for detection of landslide areas such as differentiation with edge enhancing filters [3], texture feature extraction [4], vegetation index utilized land cover change detection method [5], 3D stereo pair of images utilized change detection method [6], etc. Also, satellite remote sensing based rainfall rate estimation methods are proposed and discussed [7]-[10].

It is well known that laser ranging instrument allows mm order of movement from several 10m far from the target. It, however, is affected by rainfall. Rain droplet reflect and scattered the laser light. Therefore, previous system utilized time diversity method. Namely, if rain droplets are situated in between laser ranging instrument and the target, received signal returned faster than that without rain droplet. Therefore, the longest time duration between laser light emission and receiving the return signal from the target corresponds to the distance between laser ranging instrument and the target. Thus, influence due to rain droplets can be reduced. Although the sensor network for landslide monitoring with laser ranging system avoiding rainfall influence on laser ranging by means of time diversity and satellite imagery data based landslide disaster relief is proposed already, rainfall rate estimation accuracy is not good enough. Another demand for land slide monitoring is that rain type discrimination and rain droplet size distribution estimation. Droplet size and rainfall rate can be estimated. Thus, land slide detection and prediction can be done accurately.

The proposed methods for size distribution estimation and rainfall type discrimination using measured phase function make land slide detection and prediction accurately. If not only distance measurements but also observation angle dependency on the measured scattered laser light due to rain droplets is measured, then optical property, scattering characteristics of the rain droplets is estimated together with rain droplet size. Thus rain type can be estimated together with rainfall rate. The method proposed here is to estimate for both rain type and rainfall rate.

The next section describes the proposed system followed by experiment. The experiments can be divided into two are intended to show the sensitivity of solar direct and diffuse pointing angle on the aerosol parameter estimations. Then concluding remarks are described with some discussions.

II. PROPOSED METHOD

A. Research Background

F.Yoshino [11], Christian Matzler [12], and the others estimate parameters of droplet size distributions, stratiform (Marshall and Palmer), drizzling (Joss-Drizzle), thunderstorm (Joss-Thunderstorm) and realistic rainfall (Laws-Persons) by using Normalized distribution (Marshall-Palmer: MP, JossDrizzle: JD, Joss-Thunderstorm: JT and LP distributions). Typical parameters of these different types of rainfall are shown in Table 1. Droplet size distribution, on the other hand, is shown in Fig.1.

TABLE I. PARAMETERS FOR LP, MP, JD, JT DISTRIBUTIONS

Distribution	N(R)	^R	μ	Z-R	Rain_type
LP	1.98E-5R^(-0.384)	5.38R^(-0.186)	2.93	378R^1.43	Realistic
MP	8.0E-06	4.1R^(-0.21)	0	298R^1.50	Stratiform
JD	3.0E-05	5.7R^(-0.21)	0	120R^1.49	Drizzle
JT	1.4E-06	3.0R^(-0.21)	0	536R^1.48	Thunderstorm

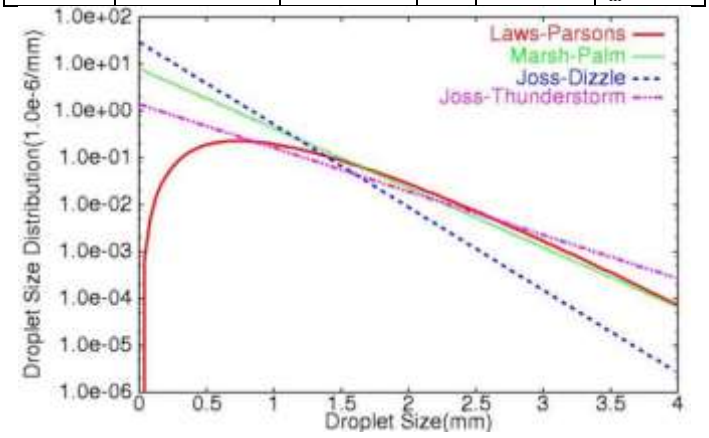

Fig. 1. Droplet size distribution of four typical rainfall models

$N(D)$ denotes droplet size distribution and is represented as equation (1) of gamma distribution function proposed by Ulbrich [13].

$$N(D)=N_0\exp(-\Lambda D^{\mu}) \quad (1)$$

where N_0 denotes N axis cross section of droplet size distribution while D denotes the factorial of power law of rain droplet size distribution. Meanwhile, μ denotes slope droplet size distribution in logarithmic-logarithmic expression. When $\mu=0$, then $D^{\mu}=1$. On the other hand, Λ defines exponential function based droplet size distribution,

$\Lambda = \alpha R^{\beta}$.

Furthermore,

$$\Lambda = 4.1 \times R^{-0.21} (mm^{-1}) \quad (2)$$

$$N_0 = 8 \times 10^3 (mm^{-1}m^{-3}) \quad (3)$$

The parameters shown in Table 1 are estimated based on Rayleigh scattering assumption. Thunderstorm is characterized as relatively large "a" and comparatively small "b" while stratiform is characterized as relatively small "a" and comparatively large "b". These estimated results are coincident to Z-R Relation[1] which is estimated by Remko Uijlenhoet et al. [14]. If we assume a certain drop size distribution (e.g., Marshall Palmer), the Z-R relation is for rain assuming a Marshal Palmer drop size distribution:

$$\Lambda = 200R^{1.6} \quad (4)$$

Next Mie scattering based Z-R Relation is estimated. In general, the number of droplets is decreasing in accordance with decreasing of droplet size [15]. From Fig.2, it is set that droplet size ranges from 1 to 6.4 mm while air temperature is assumed to be 20 degrees centigrade under the standard atmospheric pressure.

1 http://apollo.lsc.vsc.edu/classes/remote/lecture_notes/radar/conventional/ZR_relations.html

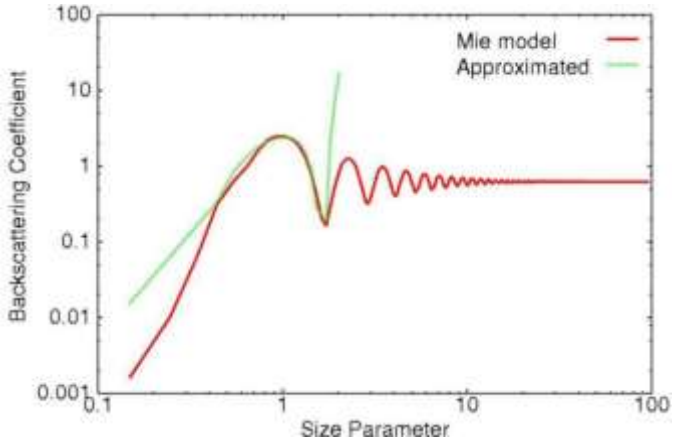

Fig. 2. Mie scattering based backscattering coefficient and its approximated coefficient

B. Optical Property

Optical property of scattered laser light by rain droplet depends on droplet size. If the droplet size is smaller than Rayleigh limitation ($\lambda/10$ where λ denotes observation wavelength), the optical property can be described by Rayleigh scattering theory. As shown in Fig.3, forward and backward scattering components are almost same.

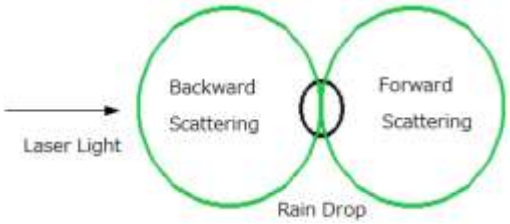

Fig. 3. Rayleigh scattering property

Therefore, phase function $P_m(\vartheta)$ of scattering property can be described as equation (5).

$$P_m(\vartheta) = \left(\frac{3}{4}\right)(1 + cos^2\vartheta) \quad (5)$$

The Rayleigh scattering of phase function is illustrated in Fig.4. On the other hand, if the droplet size is greater than Rayleigh limitation, the optical property can be described by Mie scattering theory. As shown in Fig.5, forward scattering is dominant.

Mie scattering intensity is expressed as equation (6).

$$\beta_a(\vartheta) = \frac{r^2}{2\pi}\int_{r_{min}}^{r_{max}}\{i_1(\vartheta, x, \tilde{m}) + i_2(\vartheta, x, \tilde{m})\}n(r)dr \quad (6)$$

where i_1, i_2 denotes Mie scattering intensity function as the function of x of size parameter, ϑ, and $\tilde{m}$ of rain droplet refractive index. On the other hand, $n(r)$ denotes the number of droplets of which the radius is r and is called as number of droplet particle size distribution in unit of $1/cm^2/\mu m$.

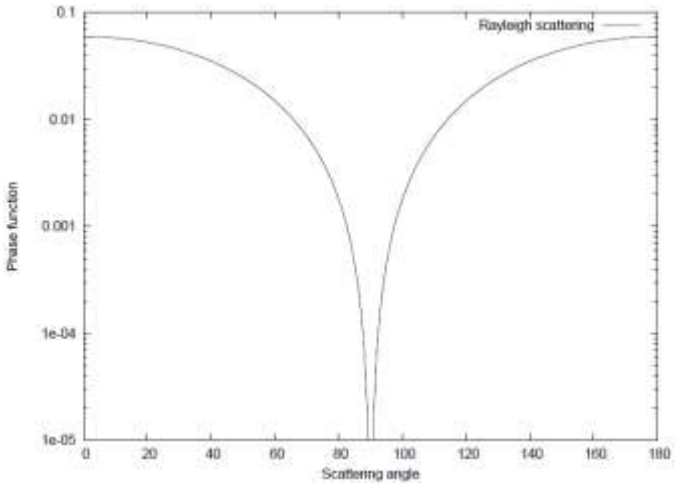

Fig. 4. Phase function of Rayleigh scattering property

Fig. 5. Mie scattering property

$$n(r) = dN(r)/dr \quad (7)$$

The size parameter can be represented as follows,

$$x = \left(\frac{2\pi}{\lambda}\right) r \quad (8)$$

The Mie scattering of phase function is illustrated in Fig.6.

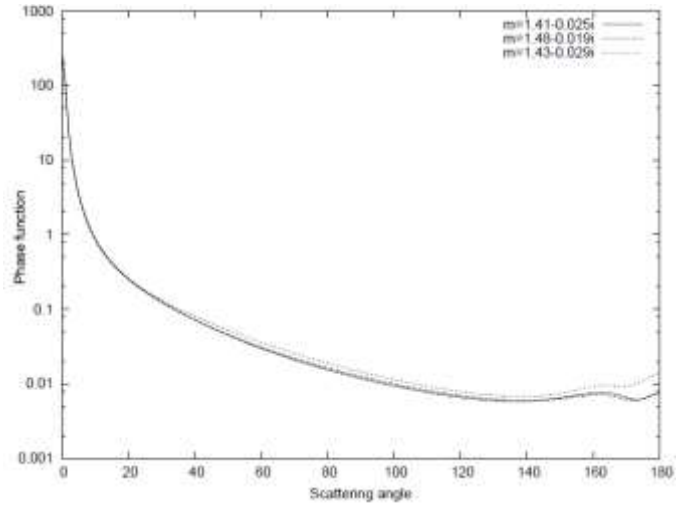

Fig. 6. Phase function of Mie scattering property

C. Simulation

For the proposed method, observation wavelength of laser light is much smaller than rain droplet size. Therefore, rain droplet scattering property can be described by Mie scattering theory. Using MODTRAN [2] of software code of radiative transfer model, phase function can be calculated. Fig.7 shows the phase function for rainfall rate of 1, 5, 10 and 15 mm/hour.

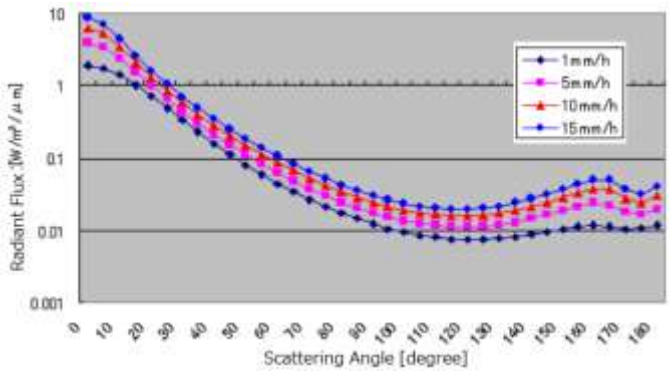

Fig. 7. Phase function of rain droplets

Therefore, it is possible to estimate rainfall rate using measured phase function. The phase function can be measured with reflected laser light intensity with the different observation angles.

III. Experiments

A. Preliminary Experiment

The configuration of the preliminary experiment is illustrated in Fig.8.

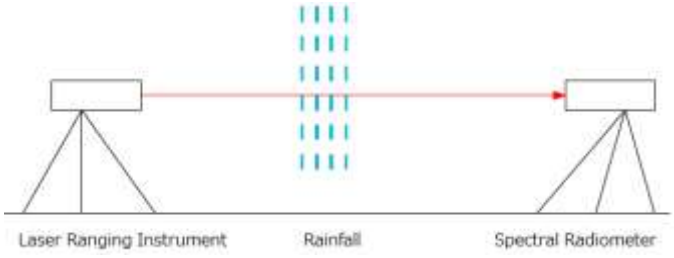

Fig. 8. Configuration of preliminary experiment

Outlook of the laser ranging instrument used is shown in Fig.9 (a) while that of the spectral radiometer is shown in Fig.10, respectively. Meanwhile, major specifications of the laser ranging instrument LEICA DISTO A6[3] and the spectral radiometer MS-720[4] are shown in Table 2 and 3, respectively.

TABLE II. Major Specification of Laser Ranging Instrument of LEICA DISTO A6

Measurable_range	0.05m~200m
Accuracy	±1.5mm
Laser_color	Red
Laser_wavelength	620-750nm

[2] https://en.wikipedia.org/wiki/MODTRAN
[3] http://distagage.us/distoa6.html
[4] http://eko.co.jp/meteorology/met_products/0015.html

TABLE III. MAJOR SPECIFICATION OF MS-720

Wavelength_Coverage	350～1,050nm
Wavelength_Interval	3.3nm
Wavelength_Resolution	10nm
Wavelength_Accuracy	<0.3nm
Full_Aparture	180°
StrayLight	<0.15%
Temperature_Dependency	±5%
Output_Unit	W/m²/μm_or_μmol/m²/s/μm
Measuring_Interval	0.005～5sec(Automatic adjustment)

(a) Laser ranging instrument

(b) Spectral radiometer

Fig. 9. Outlook of laser ranging instrument and spectral radiometer used for the preliminary experiment

Fig.10 (a) shows spectral response measured with the spectral radiometer under the rainy condition. The wavelength of the laser ranging instrument is 630 nm.

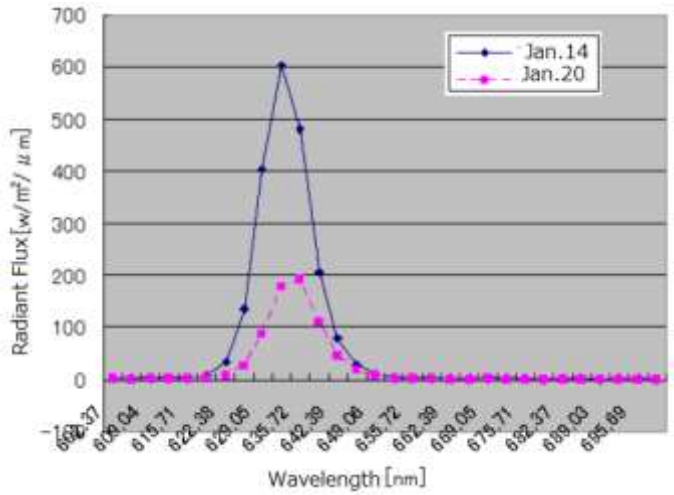

(a) Rainy condition in the nature

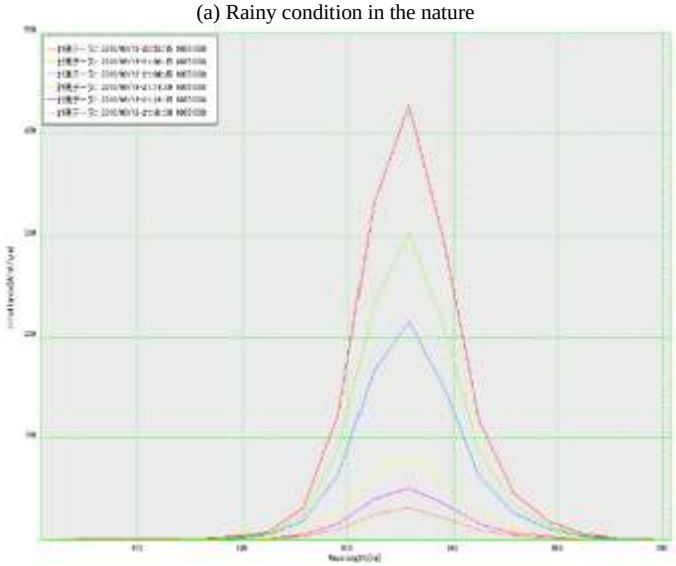

(b) Artificial rainy condition (0,2.3,4.5,9, 18, 27 mm/houor)

Fig. 10. Spectral response of the laser ranging instrument

The preliminary experiment is conducted for no rainfall condition on January 14 and 20 in 2012. Meanwhile, Fig.10 (b) shows the spectral radiometer responses for artificial rainy condition of rainfall rate of 0, 2.3, 4.5, 9, 18, and 27 mm/hour.

Therefore, there is peak at the laser wavelength.

On the other hand, Fig.11 shows the measured phase function. By changing the angle between laser light directions and pointing angle of the spectral radiometer, phase function can be measured as shown in Fig.12.

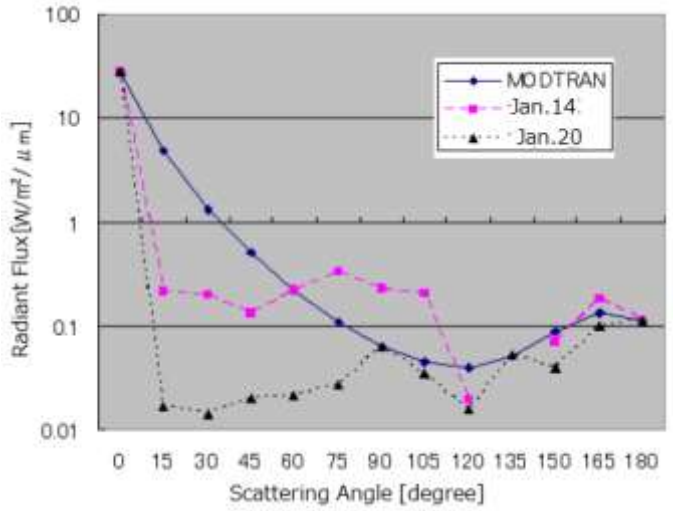

Fig. 11. Measured phase function

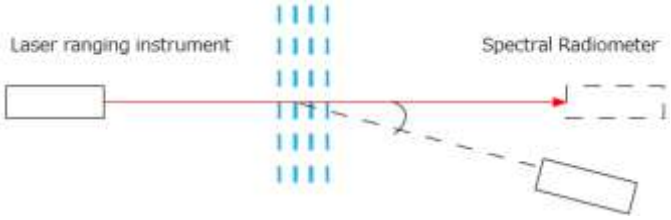

Fig. 12. Configuration of preliminary experiment (Phase function)

B. Experiment for the Different Rainfall Conditions

Experimental configuration is shown in Fig.13.

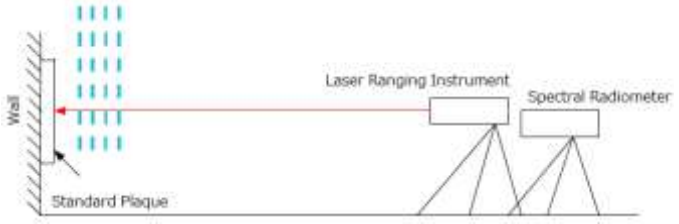

Fig. 13. Configuration of preliminary experiment

Fig.14 shows the measured spectral radiant flux of the scattered laser light from the back for no rainfall condition. Red line shows the radiant flux without laser light (noise component). Therefore, it is found that MS-720 of spectral radiometer is so noisy for the wavelength is over 900 nm. On the other hand, blue and green lines show laser repetition cycle 1 and 3 seconds, respectively. There are some water vapor and O_2 absorption lines in the Fig.14 of spectral radiant flux. Also, red laser light is not so dominant for the scattered light. Furthermore, 3 seconds repetition cycle response is a little bit greater than that for 1 second repetition cycle.

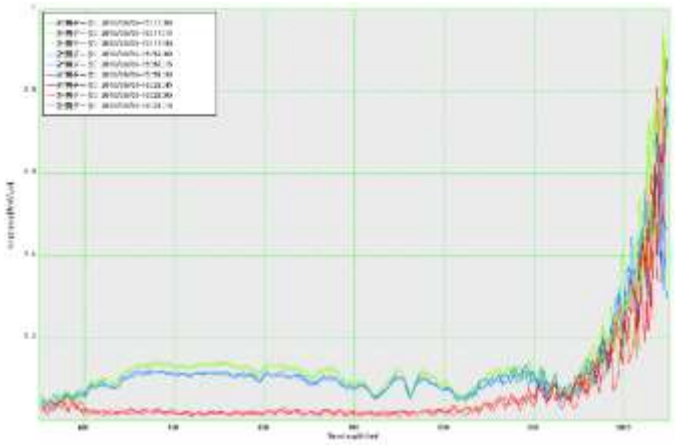

Fig. 14. Spectral radiant flux of the scattered laser light from the back for no rainfall condition

Fig.15 (a) shows the measured spectral radiant flux of the scattered laser light from the back for rainy condition. Rainfall rate for this case is 9 mm/hour. Red and green lines show laser repetition cycle 1 and 3 seconds, respectively. Through the comparison between Fig.14, it is found that the response for the 9mm/hour of the rainfall rate is a little bit lower than that for no rainfall condition obviously. Meanwhile, Fig.15 (b) and (c) shows the measured spectral radiant flux of the scattered laser light from the back for rainy condition. Rainfall rate for this case is 18 and 27 mm/hour, respectively.. Red and green lines show laser repetition cycle 1 and 3 seconds, respectively. Through the comparison between Fig.14, it is found that the response for the 18 and 27 mm/hour of the rainfall rate is a little bit lower than that for no rainfall condition obviously.

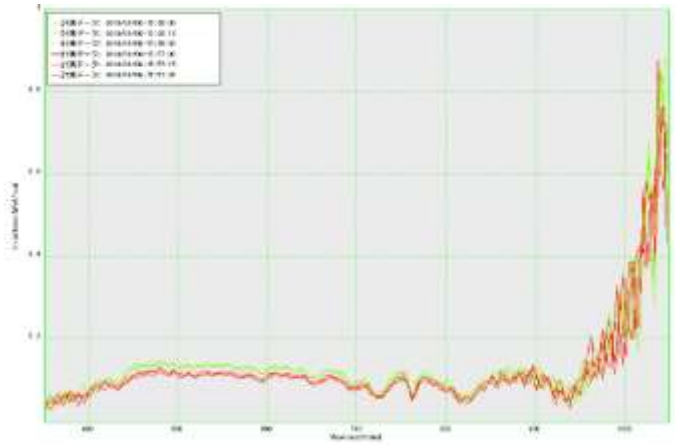

(a) (9 mm/hour)

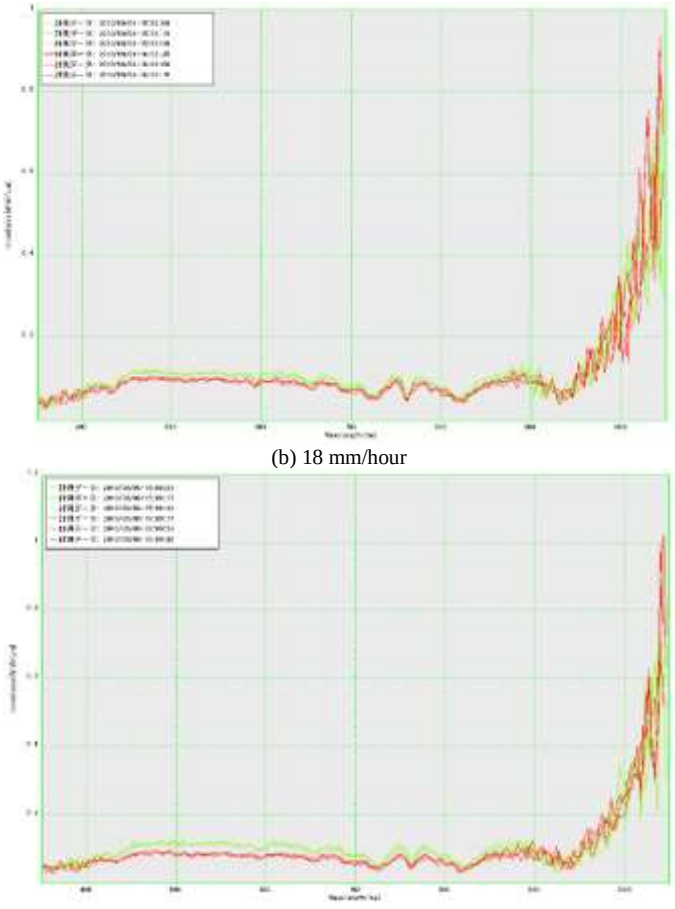

(b) 18 mm/hour

(c) 27 mm/hour

Fig. 15. Spectral radiant flux of the scattered laser light from the back for rainy condition

On the other hand, Fig.16 (a) and (b) shows the measured spectral radiant flux of the scattered laser light from the back for no rainy and rainy conditions. Laser repetition cycle is set at 1 second for Fig.16 (a) while that for Fig.16 (b) is set at 3 seconds, respectively. Red, green, blue and violet lines in Fig.16 show the cases of rainfall rate of 0, 9, 18, and 27 mm/hour, respectively.

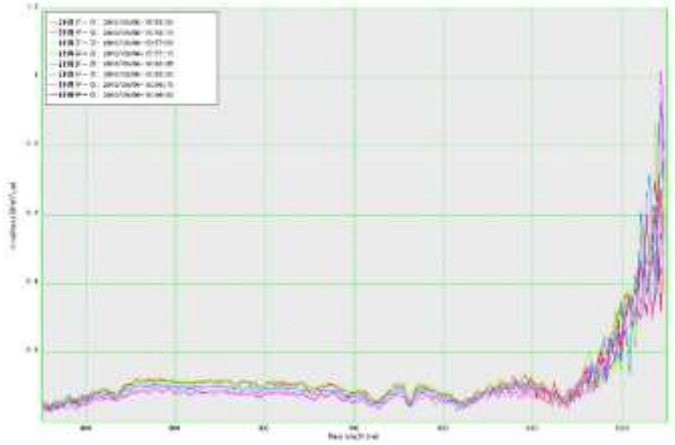

(a) 1 second

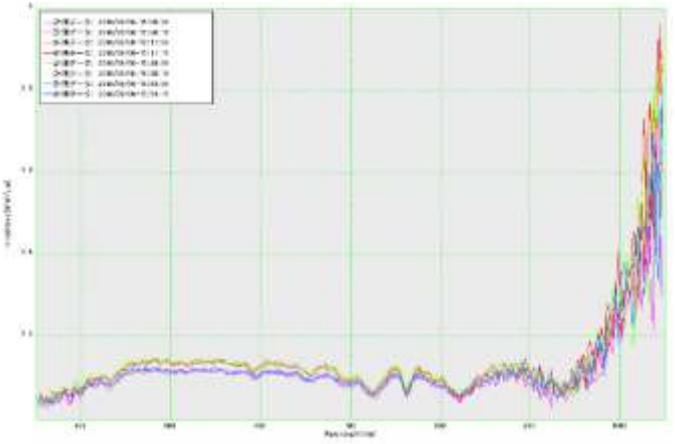

(b) 3 seconds

Fig. 16. Spectral radiant flux of the scattered laser light from the back for no rainfall and rainy conditions

It is confirmed that the repetition cycle of 3 seconds would be better to get much high sensitivity of the scattered laser light from rain droplets.

IV. Conclusion

Methods for size distribution estimation and rainfall type discrimination with estimated phase function using measured reflected laser light by rain droplet are proposed. Preliminary experiments are conducted with Laser ranging instrument and spectral radiometer for estimation of size distribution and rainfall type discrimination as well as phase function of scattering by rain drops.

Through the experiments, it is found that rainfall type can be discriminated with the measured phase function using laser light scattered by rain droplets. Also, it is found that rain droplet size distribution can be estimated with the same measured phase function. Furthermore, rainfall rate is also estimated with the response of the scattered laser light by rain droplets.

Further investigation is highly required for the experiments in real situations. Also, relation between rainfall rate and land slide has to be clarified. Although the sensor network for landslide monitoring with laser ranging system avoiding rainfall influence on laser ranging by means of time diversity and satellite imagery data based landslide disaster relief is proposed already, rainfall rate estimation accuracy is not good enough.

Acknowledgements

Author would like to thank Mr. Kiyohito Kawasaki of former student of Saga University for his effort for conducting the experiments.

References

[1] Dunnicliff, J. 1993. Geotechnical Instrumentation for Monitoring Field Performance. New York: John Wiley & Sons

[2] Mikkelsen, P.E. 1996. Field instrumentation. In A.K. Turner & R.L. Schuster (eds), Landslides: Investigation and Mitigation, Special Report 247: 278–316. Washington, DC: National Academy Press.

[3] Eyers, R., Moore, J. McM., Hervas, J. and Lui, J. G., 1995. Landslide mapping using digital imagery: a case history from south east Spain".

Proc. 31st Annual Conf. on Geohazards and Engineering Geology, 379 – 388. 1995, Coventry, UK

[4] Wang, L. and He, D. C. "A new statistical approach for texture analysis". Photogrammetric Engineering and Remote Sensing, 56 (1), 61 – 66. 1990.

[5] Zhang, Z.; Gong, H.; Zhao, W.; Zhang, Y. 2005. AppLeication of remote sensing to study of landslides. IEEE, 1546-1549.

[6] Rosin, P.L. and Hervás, J. (2005). Remote sensing image thresholding methods to determining landslide activity. International Journal of Remote Sensing, 26, 6, 1075-1092

[7] Kohei Arai, Xing Ming Liang, Comparison of rainfall rate using TRMM satellite onboard PR data derived from Rayleigh and Mie scattering assumptions and Z-R relation assumption, Journal of Japan Society of Photogrammetry and Remote Sensing, 49, 2, 67-74, 2010

[8] Kohei Arai, Kenta Azuma, Rainfall rate estimation with AMSR data on board AQUA satellite taking into account geometric relation between the microwave radiometer and observation targets, Journal of Japan Society of Photogrammetry and Remote Sensing, 49, 1, 32-40, 2010

[9] K.Arai, Sensor network for landslide monitoring with laser ranging system avoiding rainfall influence on laser ranging by means of time diversity and satellite imagery data based landslide disaster relief, International Journal of Applied Sciences, 3, 1, 1-12, 2012.

[10] Kohei Arai, Comparison between Rayleigh and Mie scattering assumptions for Z-R relation and rainfall rate estimation with TRMM/PR data, International Journal of Advanced Research in Artificial Intelligence, 2, 8, 1-6, 2013.

[11] F.Yoshino, Radar Hydrology, MorikitaShuppan Publishing Co. Ltd, 2002.

[12] C. Mätzler, Drop-Size Distributions and Mie Computations for Rain,InstitutfürAngewandtePhysik, Research Report No. 2002-16, 2002

[13] C.W. Ulbrich, Natural Variations in the Analytical Form of the Raindrop Size Distribution, Journal of Applied Meteorology, 22(10), pp.17641775, 1983.

[14] U. Remko, Raindrop size distributions and radar reflectivity–rain rate relationships for radar hydrology, Hydrology and Earth System Sciences, 5(4), pp.615-627, 200

[15] L.J. Battan, Radar Observation of the Atmosphere, Univ. of Chicago Press, Chicago, Illinois, 324p., 1973.

AUTHORS PROFILE

Kohei Arai, He received BS, MS and PhD degrees in 1972, 1974 and 1982, respectively. He was with The Institute for Industrial Science and Technology of the University of Tokyo from April 1974 to December 1978 and also was with National Space Development Agency of Japan from January, 1979 to March, 1990. During from 1985 to 1987, he was with Canada Centre for Remote Sensing as a Post-Doctoral Fellow of National Science and Engineering Research Council of Canada. He moved to Saga University as a Professor in Department of Information Science on April 1990. He was a counselor for the Aeronautics and Space related to the Technology Committee of the Ministry of Science and Technology during from 1998 to 2000. He was a councilor of Saga University for 2002 and 2003. He also was an executive councilor for the Remote Sensing Society of Japan for 2003 to 2005. He is an Adjunct Professor of University of Arizona, USA since 1998. He also is Vice Chairman of the Commission-A of ICSU/COSPAR since 2008. He received Science and Engineering Award of the year 2014 from the minister of the ministry of Science Education of Japan and also received the Bset Paper Award of the year 2012 of IJACSA from Science and Information Organization: SAI. In 2016, he also received Vikram Sarabhai Medal of ICSU/COSPAR and also received 20 awards. He wrote 34 books and published 520 journal papers. He is Editor-in-Chief of International Journal of Advanced Computer Science and Applications as well as International Journal of Intelligent Systsems and Applications. http://teagis.ip.is.saga-u.ac.jp/

Data Hiding Method Replacing LSB of Hidden Portion for Secret Image with Run-Length Coded Image

Kohei Arai[1]
[1]Graduate School of Science and Engineering
Saga University
Saga City, Japan

***Abstract*—Data hiding method based on steganography improving secret image invisibility through replacing Least Significant Bit: LSB with run-length coded Image is proposed. Although, the proposed method is based on Discrete Wavelet Transformation: DWT, run-length coded secrete image is embedded in the LSB of the high frequency component before reconstruction of the image for opening to the public for improvement of the secrete image invisibility. Before embedding the coded secret image, the coded secret image bits are rearranged the order by using random number. Therefore, secret image invisibility is much improved. Through experiments, it is confirmed that secret images are almost invisible in distribute images. Data hiding performance in terms of invisibility of secret images which are embedded in distribute images is evaluated with the Peak Signal to Noise Ratio: PSNR and the Root Mean Square: RMS difference between the original secret image and extracted one from the distribute images. Meanwhile the conventional Multi-Resolution Analysis: MRA based data hiding is attempted with a variety of parameters, level of MRA and the frequency component location of which secret image is replaced to it and is compared to the proposed method. It is found that the proposed data hiding method is superior to the conventional method.**

Keywords—Wavelet; DWT; Steganography; Random number based Permutation; Data hiding; Data compression

I. INTRODUCTION

Wavelet analysis applications are getting more popular in time series analysis, image analysis, information security area, etc.[1],[2]. Data hiding is important for information contents security, in particular, for protection of copy right. Using data hiding methods, some important information such as copyright, signature, etc. can be embedded. Data hiding based on wavelet analysis, in particular, Multi-Resolution Analysis: MRA is widely used. One of the problems on data hiding methods is visibility of the embedded information on the available distribute images [3]-[7]. The other problem is robustness against image processing which is applied to the distribute images including data compressions. It sometime occurs that small amount of information on the embedded image appears on the distribute images slightly due to the embedding mechanism of the data hiding.

In order to improve invisibility of the secret images in the distribute images, run-length coded binarized secret images are used. The locations of the codes after the data compression in one of the frequency component images after the dyadic wavelet transformation [8] are determined with random numbers generated by Mersenne Twister of random number generator. After all, reconstructed image (inverse dyadic wavelet transformation) is used for distribute images. The original secret images are almost invisible in the distribute images. Although the method for data hiding based on Legall 5/2 (Cohen-Daubechies-Feauveau: CDF 5/3) wavelet with data compression and random scanning of secret imagery data is proposed [9], invisibility of the secret image is not good enough. Therefore, improvement of the invisibility is still required.

This paper deals with the current problems on the widely used MRA based data hiding method (Conventional data hiding method). One of the problems is visibility of secret image in the distribute images followed by robustness against distribute image manipulations including image deformation, geometric conversion, data compression, etc. In order to overcome the aforementioned problems, a method for data hiding based on lifting dyadic wavelet transformation with run-length coding of data compression which is applied to secret image together with pixel order exchange is proposed. This is well reported in the previously published paper [10]. The method proposed is to improve the invisibility of the secret images by using the process of which the run-length coded secret image is replaced to several bits from the Least Significant Bit: LSB of one of the decomposed images. It is called as "Steganography" that the coded secret image is embedded in the LSB. LSB is not so visible. Therefore, embedding the coded secret image in the LSB implies improvement of secret image invisibility. Before replace the secret image to one of the decomposed components of the original image, secret image is encoded by run-length coding with Modified Huffman code. Then the coded image is scanned with the random numbers generated with Mersenne Twister and is replaced to the one decomposed components with the information of compressed image size, initial value of the random number and the parameters of wavelet transformation based on lifting dyadic wavelet. Thus the secret image becomes invisible.

First, the aforementioned problems of the conventional MRA based data hiding method are described followed by the proposed method. Then it is enhanced that the proposed

method achieved significantly improvement of invisibility of the secret images through experiments with the standard image database for data compression performance evaluations.

II. Proposed Method

A. Conventional Data Hiding Method Based on Discrete Wavelet Transform

Wavelet utilized MRA allows decompose the image with wavelet coefficients (high and low frequency components) and also the original image can be reconstructed with the decomposed wavelet coefficients perfectly. If the high frequency component is replaced with secret image to be hidden, and if the reconstructed image is distributed to public, then secret image can be extracted from the distributed image if receiver knows which component is replaced with secret image. In this case, secret image has to be invisible in the distributed image. Also even if image processing including geometric conversion (linear transformation) and data compression (nonlinear transformation) is applied to the distributed image, secret image has to be extracted. The aforementioned "invisibility" and "robustness against image processing" are very important for data hiding.

The proposed method for data hiding is based on dyadic wavelet transformation. Dyadic wavelet allows to separate frequency components keeping image size with that of original image. Dyadic wavelet is called as a binary wavelet and has high pass and low pass filter components, $\{h[k], g[k]\}$ and reconstruction filter $\{h[k], g[k]\}$. Low and high frequency components, c_n and d_n are expressed as follows,

$$c_n[i]=\Sigma_k h[k]C_{n-1}[i+k_{2n-1}] \quad (1)$$

$$d_n[i]=\Sigma_k g[k]C_{n-1}[i+k_{2n-1}] \quad (2)$$

Then original image is also reconstructed with the low and high frequency components as follows,

$$c_{n-1}[i]=1/2\Sigma_k h[k]c_n[i-k2^{n-1}]+\Sigma_k g[k]d_n[i-k2^{n-1}] \quad (3)$$

If a new parameter s[m] is employed, then lifting dyadic wavelet is defined as follows,

$$h^{new}[k]=h^{old}[k] \quad (4)$$

$$h^{new}[k]=h^{old}[k]+\Sigma_m s[-m]\, g^{old}[k-m] \quad (5)$$

$$g^{new}[k]=g^{old}[k]-\Sigma_m s[m]\, h^{old}[k-m] \quad (6)$$

$$g^{new}[k]=g^{old}[k] \quad (7)$$

In Fig.1, the secret binary image of Mandrill [11] with a certain threshold is embedded in the HL component of the dyadic wavelet transformed images derived from the original image of Lenna [11] with dyadic wavelet transformation. At the left bottom corner of Fig.1, a reconstructed image (image for circulation) is shown. The secret image can be recognizable in the circulation image, unfortunately. In these cases, Daubechies wavelet base function (support length=2) [12] is used. On the other hand, Fig.1 (b),(c),(d) shows reconstructed images of Mandrill of secret image (a) embedded Lenna of original images of which the secret image is embedded at the LH, HH, and HL of frequency components, respectively. Image size is not changed for original and dyadic wavelet transformed images.

B. Problem Description

Fig.2 shows a schematic process flow of the proposed data hiding based on lifting dyadic wavelet transformation. It is possible to hide the embedded image at the certain location of wavelet transformation images then distribute images containing the embedded image can be reconstructed through inverse wavelet transformation. In this case, although binary secret images are assumed, half tone, colored images are also available for secret images.

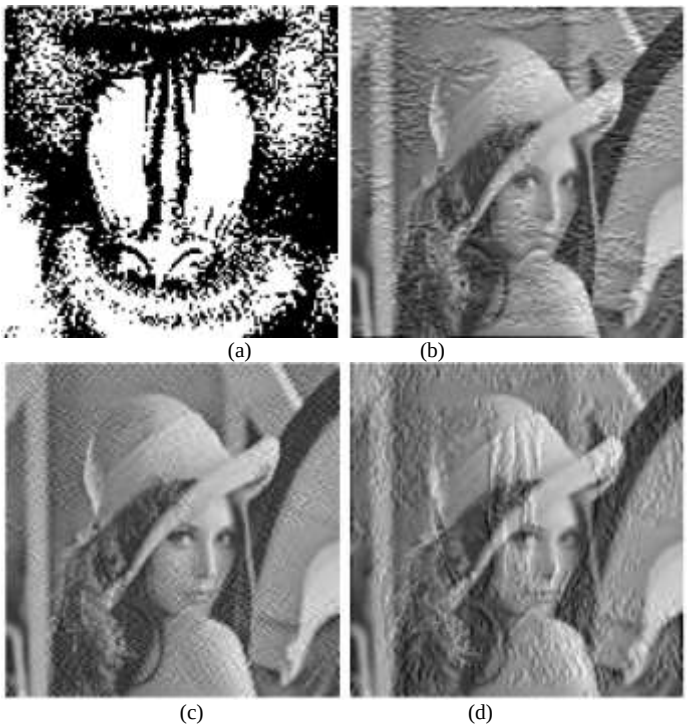

Fig. 1. (a) The binalized secret image of Mandrill, (b) Reconstructed image of Mandrill image embedded (LH) Lenna image for circulation, (c) Reconstructed image of Mandrill image embedded (HH) Lenna image for circulation, (d) Reconstructed image of Mandrill image embedded (HL) Lenna image for distribution (Image size of the secret and the reconstructed images are 128 by 128 pixels and quantization bit.is 8 for both images)

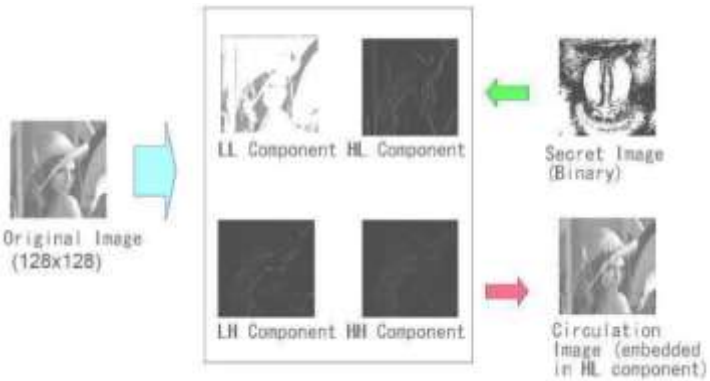

Fig. 2. Schematic process flow of the proposed data hiding

Root Mean Square: RMS difference between original and the reconstructed images is used for the evaluation of data hiding performance. The parameters of the wavelet transformation are (1) Basis function, (2) Frequency component in which the secret image is replaced, (3) Level of the wavelet transformation (wavelet transformation can be applied recursively. The number of recursive corresponds to filter bank frequency) and (4) Downsizing parameter (Dyadic wavelet transformation makes downsizing parameter is one while downsizing parameter of the ordinal wavelet transformation is used to be 1/2). Fig.3 shows RMS difference of a variety of parameters of wavelet transformation based data hiding. Fig.3 (a) shows one of examples of reconstructed image of the data hiding method with dyadic wavelet transformation while Fig.3 (c) shows another example of the reconstructed image of the data hiding method with the conventional Daubechies wavelet transformation. Meanwhile, RMS difference between the original image and the reconstructed images for the dyadic wavelet transformation based data hiding is shown in Table 1 while that for the conventional Daubechies wavelet transformation is shown in Table 2. In Fig.3, Lv1 denotes level 1 while Dbx denote Daubechies base function with support length of x.

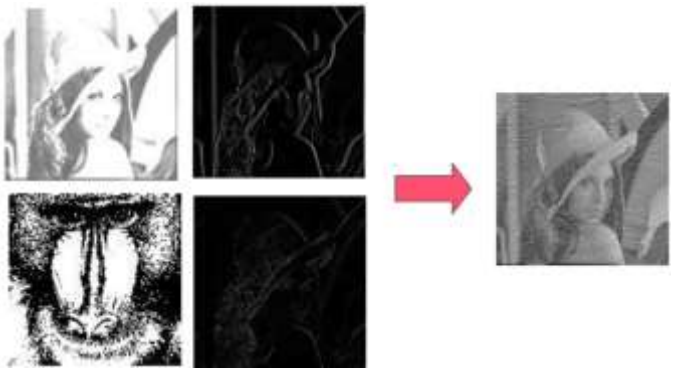

(a) Dyadic Wavelet

(b) Daubechies wavelet

Fig. 3. RMS difference of a variety of parameters of wavelet transformation based data hiding

TABLE I. RMS DIFFERENCE FOR DYADIC WAVELET BASED DATA HIDING

Lv1	Db1	Db2	Db4
LH	22.93	22.54	22.32
HH	20.5	20.38	20.3
HL	23.66	22.86	22.56

TABLE II. RMS DIFFERENCE FOR DAUBECIES WAVELET BASED DATA HIDING

Lv1	Db1	Db2	Db4
LH	80.2	79.37	79.59
HH	80.22	79.51	79.74
HL	80.89	79.87	80.12

It is quite obvious that the dyadic wavelet transformation based data hiding method is superior to the conventional Daubechies wavelet based data hiding method.

C. Previously Proposed Data Hiding Method

First, secret image is binarized. It is usual that secret images are used to be authorization images for protection of original image content (copyright). Before binarized secret images are replaced to one of the high frequency component images, run-length coding is applied to secret images in order to improve an invisibility of the secret images in the distribute images. Fig.4 shows schematic process flow of the run-length coding method. The number of pixels in the original binary image is 27 while the number of pixels in the compressed image is just 6 (quantization level is variable).

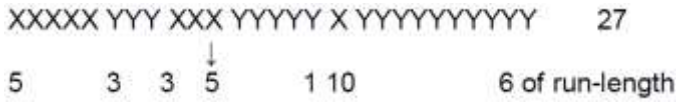

Fig. 4. Schematic process flow of run-length coding

Then run-length coded data are replaced to one of the high frequency components with the pixel order exchanges based on generated random numbers which are generated by Mersenne Twister. Only if the receiver who knows the initial value of random number of Mersenne Twister and how to decode run-length coding, then such the receiver can extract the secret images. Thus the copyright holders can assert their copy right through extraction of secret images. It, however, is not enough in terms of invisibility of the secret image.

D. Proposed Data Hiding Method

Fig.5 shows the process flow of the proposed data hiding (hide the secret image into the original image and create distribute image embedded the secret image then extract the secret image from the distribute image)

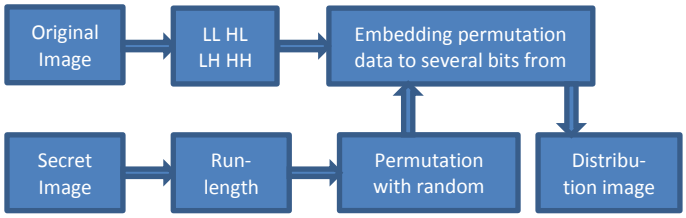

Fig. 5. Process flow of the proposed method

The method proposed is to improve the invisibility of the secret images by using the process of which the run-length coded secret image is replaced to several bits from the Least Significant Bit: LSB of one of the decomposed images derived from DWT. Several bits from LSB is almost invisible in the one of the high frequency components in the decomposed images based on DWT of wavelet transformation. Before replace the secret image to one of the decomposed components of the original image, secret image is encoded by run-length coding with Modified Huffman code which is shown in Fig.6.

Modified Huffman code consists of terminating code and make-up code and End of Line: EOL. An example is shown in the bottom of Fig.6.

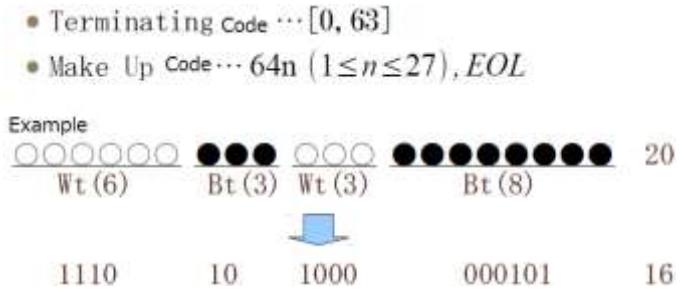

Fig. 6. Modified Huffman coding

Then the coded image is scanned with the random numbers generated with Mersenne Twister and is replaced to the one decomposed components with the information of compressed image size, initial value of the random number and the parameters of wavelet transformation based on lifting dyadic wavelet. All the required information for reconstruction of the secret image, such as wavelet transformation parameters, compressed image data size and the initial value of the random number generator are stored in several bits from the LSB of the one of the decomposed image of high frequency component of the secret image. Thus the secret image becomes much invisible in comparison to the previously proposed method.

III. EXPERIMENTS

A. Data Used

"Lenna" in the SIDBA image database is used for the original image while "Shuttle cock" and "Mandrill" in the SIDBA image database is used for the secret images. Fig.7 shows the original and the secret images. The 8-bits secret image is represented as 8 bit-plane (binary data). Each bit-plane can be encoded with run-length coding. The coded data is embedded in several bits of HH component image derived from DWT. In this process, pixel order is permutated with random number derived from Merssene Twister.

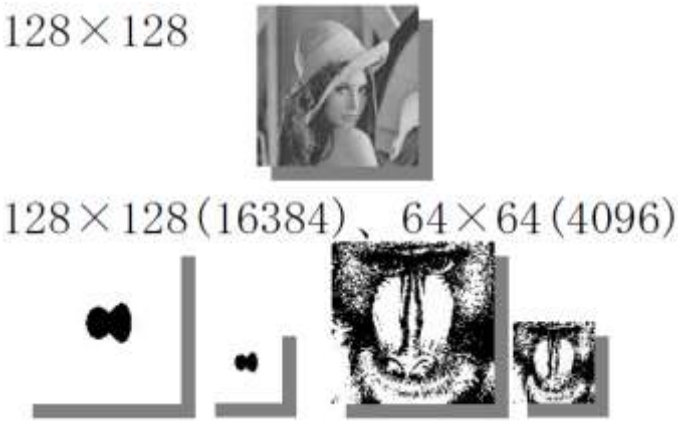

Fig. 7. Original (Top) and secret images (Bottom) used for the experiments

Not only RMS difference, but also the following Peak Signal to Noise Ratio: PSNR in unit of dB is evaluated in the experiments.

$$PSNR=20\log_{10}(Max/RMSE) \quad (8)$$

where Max=255 (8-bit quantization) and RMSE denote RMS difference between the original and the reconstructed images.

B. Preliminary Experimental Results

Level 1 of wavelet transformation is applied to the original image with dyadic and the conventional Daubechies based wavelet transformations. The secret images are replaced to the high frequency components, LH, HL, and HH after the wavelet transformation. Then the image is reconstructed for evaluation of PSNR. Fig.8 shows the evaluation results of PSNR and data size as a function of the number of pixels of the secret image size ranged from 4 to 256.

PSNR shows a peak at the secret image size of 8. Then the evaluated PSNR decreases in accordance with the increasing of the secret image size. Also it is found that HH component is most appropriate component in which the encoded secret image inserted to LSB of the HH component. Furthermore, it is found that dyadic wavelet transformation based data hiding is superior to the conventional Daubechies wavelet transformation based data hiding.

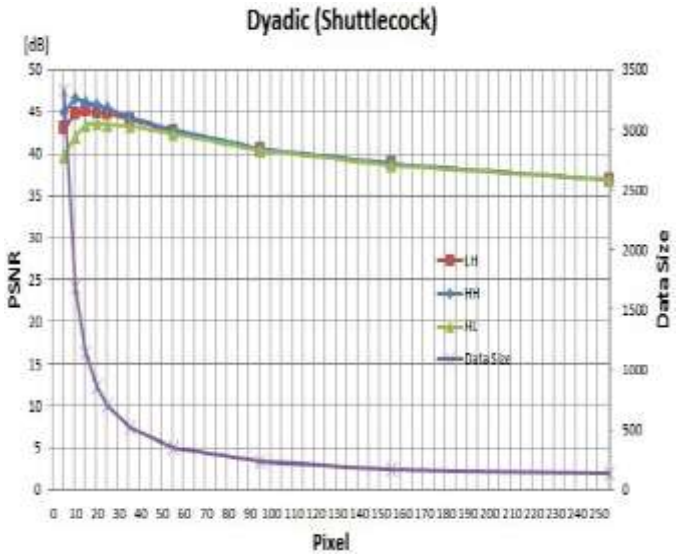

(a)

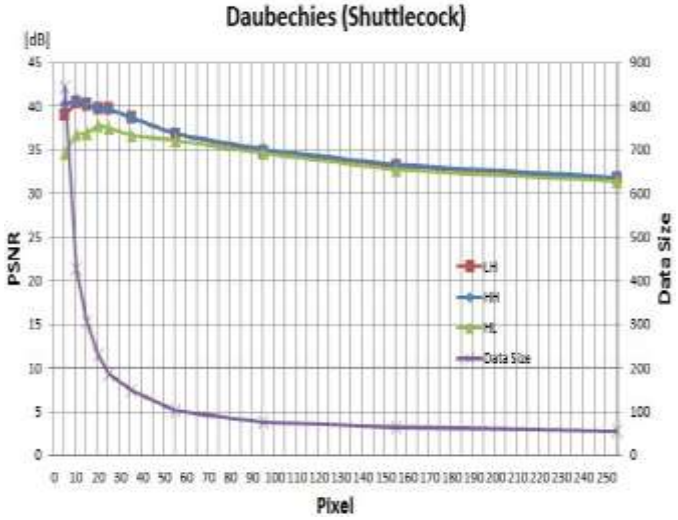

(b)

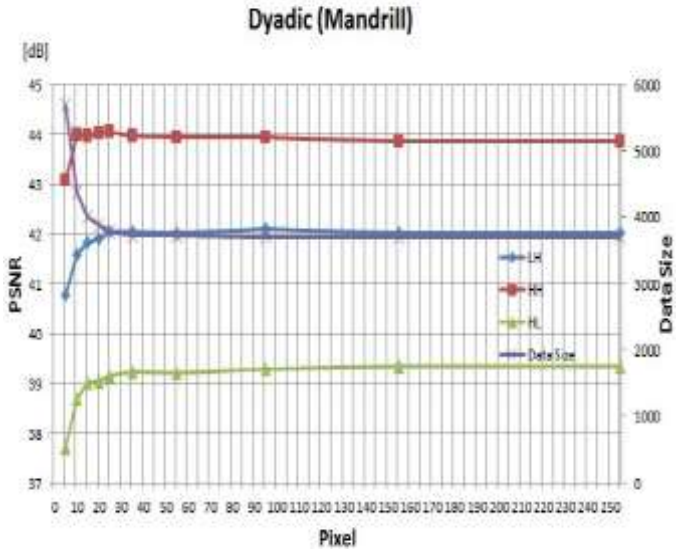

(c)

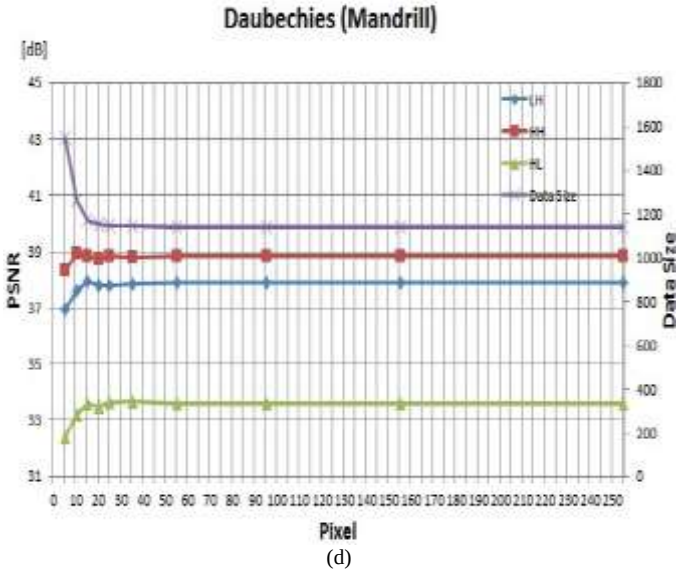

(d)

Fig. 8. Evaluation results of PSNR and data size as a function of the number of pixels ranged from 4 to 256

C. Influence Due to Threshold

The secret image of "Mandrill" is 8-bit quantized image. Therefore, data hiding performance, in terms of invisibility of the secret image depends on the threshold used for generation of the secret image.

Fig.9 shows the HH component image (on the left) and the reconstructed image (on the right). PSNR for the threshold= 255 is 36.90 dB while that for the threshold=15 is 45.16 dB. Meanwhile, the number of data for the threshold=255 is 133 while that for the threshold=15 is 1140. Therefore, it is better to select the most appropriate threshold before applying data hiding.

D. Comparison Between with and without LSB Insertion

There are two different proposed data hiding methods, with and without LSB insertion. Namely, the proposed method seems to be worked without LSB insertion. The data hiding method without LSB insertion is called standard method (STD) while that with LSB insertion is called LSB insertion method (LSB). "Shuttle cock" and "Mandrill" of the secret images are quantized with quantization bit ranged from 4 to 32.

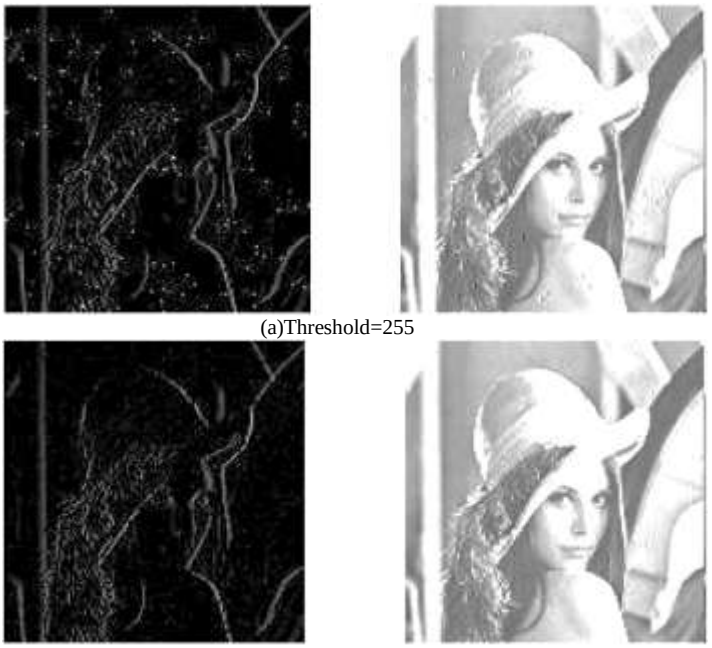

(a)Threshold=255

(b)Threshold=15

Fig. 9. Influence due to the threshold

Then the quantized secret images are encoded with run-length coding. After that the proposed data hiding methods with and without LSB insertion is applied. PSNR is evaluated for the proposed methods, with and without LSB insertion. Fig.10 shows the secret images. Table 3, 4 shows the evaluated PSNR for the secret image of Shuttle cock and Mandrill, respectively. In accordance with increasing of the number quantization bit, the number of hidden data is decreased obviously. Also, PSNR decreases in accordance with increasing of the quantization bit for the proposed data hiding method with LSB insertion while PSNR does not depend on the data hiding method without LSB insertion. Furthermore, PSNR of the data hiding method with LSB insertion is superior to the data hiding method without LSB insertion. Therefore, it is better to select the data hiding method with LSB insertion with a small quantization bit.

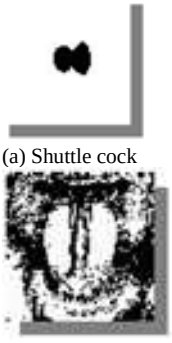

(a) Shuttle cock

(b) Mandrill

Fig. 10. Secret images

TABLE III. PSNR FOR THE PROPOSED DATA HIDING METHODS, WITH AND WITHOUT LSB INSERTION (SHUTTLE COCK)

Type#1	Hidden_Data	STD	LSB
4bir	1395	38.59	52.12
8bit	608	41.16	48.19
16bit	306	40.7	44.4
32bit	158	38.82	40.65

TABLE IV. PSNR FOR THE PROPOSED DATA HIDING METHODS, WITH AND WITHOUT LSB INSERTION (MANDRILL)

Type#2	Hidden_Data	STD	LSB
4bit	2085	36.85	52.14
8bit	1378	38.43	49.0
16bit	1169	38.71	45.33
32bit	1147	38.63	42.84

E. Evaluation of the Proposed Method

Another dataset is prepared as shown in Fig.11. The original images, "Lenna" and "Bridge" are 128 by 128 pixels of 8-bit quantized greyscale images while the secret images, "Barbra" and "SIDBA Title" are 32 by 32 pixels of 8-bit quantized greyscale images.

Fig. 11. Original and secret images used for the experiments

In accordance with the procedure of the proposed data hiding method, the secret images, Barbra and SIDBA-Title are embedded in the original image, Lenna and Bridge. In case of Barbra is embedded in the original images, data compression ratio is 71.76% (Fig.12 (a)) while SIDBA-Title is embedded in the original images, data compression ratio is 65.92% (Fig.12 (b)).

PSNR for these cases are shown in Table 5.

TABLE V. PSNR FOR THE PROPOSED DATA HIDING METHOD

PSNR	Lenna	Bridge
Barbra	46.83	47.21
SIDBA-Title	46.90	47.40

PSNR for all the cases are over 46 dB and are beyond the preliminary case studies. Therefore, it may conclude that the secret images are almost invisible.

(a)"Barbra"

(b)"Sidba-Title

Fig. 12. Distribution images for the cases that Barbra and SIDBA-Title is embedded in the original images

IV. CONCLUSION

Data hiding method based on steganography improving secret image invisibility through replacing Least Significant Bit: LSB with run-length coded Image is proposed. Lifting dyadic wavelet is used for fundamental data hiding. Although, the proposed method is based on Discrete Wavelet Transformation: DWT, run-length coded secrete image is embedded in the LSB of the high frequency component before reconstruction of the image for opening to the public for improvement of the secrete image invisibility. Before embedding the coded secret image, the coded secret image bits are rearranged the order by using random number. Therefore, secret image invisibility is much improved.

Through experiments, it is confirmed that secret images are almost invisible in distribute images. Data hiding performance in terms of invisibility of secret images which are embedded in distribute images is evaluated with the Peak Signal to Noise Ratio: PSNR and the Root Mean Square: RMS difference between the original secret image and extracted one from the distribute images. Meanwhile the conventional Multi-Resolution Analysis (MRA) based data hiding is attempted with a variety of parameters, level of MRA and the frequency component location of which secret image is replaced to it and is compared to the proposed method.

It is found that the PSNR shows a peak at the secret image size of 8. Then the evaluated PSNR decreases in accordance with the increasing of the secret image size. Also it is found that HH component is most appropriate component in which

the encoded secret image inserted to LSB of the HH component. Furthermore, it is found that dyadic wavelet transformation based data hiding is superior to the conventional Daubechies wavelet transformation based data hiding. PSNR for all the cases of the experiment conducted for the proposed data hiding method are over 46 dB and are beyond the preliminary case studies. Therefore, it may conclude that the secret images are almost invisible.

Further investigations are required for utilization of relational information, shape information, and so on. Also, it is desirable to conduct a research on image retrieval based on deep learning. On the evaluation of the image quality, not only PSNR but also other measures have to be created in an realistic manner.

ACKNOWLEDGEMENTS

Author would like to thank Mr.Yuji Yamada, former Saga University student for his great effort to conduct the experiments.

REFERENCES

[1] Kohei Arai, Fundamental Theory on Wavelet Analysis, Morikita Shuppan Publishing Co. Ltd., 2000.

[2] Kohei Arai, Self Learning on Wavelet Analysis, Kindai-Kagakusha publishing Co. Ltd.. 2006.

[3] Kohei Arai and Kaname Seto, Data hiding method based on Multi-Resolution Analysis: MRA, Visualization Society of Japan, 22, Suppl.No.1, 229-232, 2002.

[4] Kohei Arai and Kaname Seto, Data hiding method with coordinate conversion in feature space, Visualization Society of Japan, 25, Suppl.No.1, 55-58, 2005.

[5] Kohei Arai and Kaname Seto, Improvement of invisibility of secret images embedded in circulate images based on MRA with coordinate conversion and Principal Component Analysis: PCA, Journal of Image and Electronics Society of Japan, 36, 5, 665-673, 2007.

[6] Kohei Arai and Kaname Seto, Improvement of invisibility of secret images embedded in circulate images based on MRA with scanning scheme conversion, Visualization Society of Japan, 29, Suppl.No.1, 167-170, 2009.

[7] Kohei Arai, Improvement of security and invisibility of secret images embedded in circulate images and based on MRA, Report of RIMS-Research Institute for Mathematical Sciences Kyoto University, ISSN188-2818,1684,93-113,2010.

[8] S.Mallat and S.Zhong, ``Characterization of signals from multiscale edges," IEEE Trans. Pattern Anal. Machine Intell., 14, pp.710-732, 1992.

[9] Kohei Arai, Method for data hiding based on Legall 5/2 (Cohen-Daubechies-Feauveau: CDF 5/3) wavelet with data compression and random scanning of secret imagery data, International Journal of Wavelets Multi Solution and Information Processing, 11, 4, 1-18, B60006 World Scientific Publishing Company, DOI: I01142/SO219691313600060, 1360006-1, 2013

[10] Kohei Arai, Yuji Yamada, Improvement of Secret Image Invisibility in Distribute Image with Dyadic Wavelet Based Data Hiding with Run-Length Coded Secret Images of Which Location of Codes are Determined with Random Number, IJARAI, Special Issue on Artificial Intelligence, 33-40, 2012.

[11] http://vision.kuee.kyoto-u.ac.jp/IUE/IMAGE_DATABASE/STD_IMAGES/ (Accessed on March 11 2011).

[12] Kohei Arai and Leland Jameson, Earth observation satellite data analysis based on wavelet analysis, Morikita-Shuppan Publishing Co., Ltd., 2001.

AUTHORS PROFILE

Kohei Arai, He received BS, MS and PhD degrees in 1972, 1974 and 1982, respectively. He was with The Institute for Industrial Science and Technology of the University of Tokyo from April 1974 to December 1978 and also was with National Space Development Agency of Japan from January, 1979 to March, 1990. During from 1985 to 1987, he was with Canada Centre for Remote Sensing as a Post-Doctoral Fellow of National Science and Engineering Research Council of Canada. He moved to Saga University as a Professor in Department of Information Science on April 1990. He was a counselor for the Aeronautics and Space related to the Technology Committee of the Ministry of Science and Technology during from 1998 to 2000. He was a councilor of Saga University for 2002 and 2003. He also was an executive councilor for the Remote Sensing Society of Japan for 2003 to 2005. He is an Adjunct Professor of University of Arizona, USA since 1998. He also is Vice Chairman of the Commission-A of ICSU/COSPAR since 2008. He received Science and Engineering Award of the year 2014 from the minister of the ministry of Science Education of Japan and also received the Bset Paper Award of the year 2012 of IJACSA from Science and Information Organization: SAI. In 2016, he also received Vikram Sarabhai Medal of ICSU/COSPAR and also received 20 awards. He wrote 34 books and published 520 journal papers. He is Editor-in-Chief of International Journal of Advanced Computer Science and Applications as well as International Journal of Intelligent Systsems and Applications. http://teagis.ip.is.saga-u.ac.jp/

Development of Decision Support System to Selection of the Blended Learning Platforms for Mathematics and ICT Learning at SMK TI Udayana

I Made Ardana[1]
Mathematics Education
Universitas Pendidikan Ganesha
Bali, Indonesia

I Putu Wisna Ariawan[2]
Mathematics Education
Universitas Pendidikan Ganesha
Bali, Indonesia

Dewa Gede Hendra Divayana[3]
Education of Information Technology
Universitas Pendidikan Ganesha
Bali, Indonesia

***Abstract*—The development of information technology is able to solve problems in various areas of life, including education. Some examples of the application of information technology in education, among others: e-learning, e-library, e-module, blended learning, and more. One school in Bali that also apply information technology in the learning process, namely SMK TI Udayana. Application forms of information technology in the learning process at SMK TI Udayana have the shape of utilization of blended learning. There are several platforms options can be used for blended learning in the learning process at SMK TI Udayana, including: Edmodo, Quipper School, Moodle, Kelase, and others. Facts show that the number of platforms that can be used for blended learning, sometimes making teachers and students get confused to choose the most suitable, especially in the process of mathematics and ICT learning at SMK TI Udayana. Based on these problems, then created of the decision support system to be able to choose a blended learning platforms that is suitable for mathematics and ICT learning at SMK TI Udayana. The methods used in this decision support system is weighted product, because it can determine blended learning platforms for mathematics and ICT learning based on the highest value obtained from the calculation of several criteria.**

***Keywords*—Blended Learning; Decision Support System; Weighted Product; Mathematics and ICT Learning**

I. INTRODUCTION

The development of information technology is able to solve problems in various areas of life, such as agriculture, medicine, pharmacy, economics, and including also the field of education. Some examples of the application of information technology in education, among others: e-learning, e-library, e-module, blended learning, and more. One school in Bali that also apply information technology in the learning process, namely SMK TI Udayana. Application forms of information technology in the learning process at SMK TI Udayana have the shape of utilization of blended learning. There are several platforms options can be used for blended learning in the learning process at SMK TI Udayana, including: Edmodo, Quipper School, Moodle, Kelase, and others. Facts show that the number of platforms that can be used for blended learning, sometimes making teachers and students get confused to choose the most suitable, especially in the learning process of Mathematics and ICT learning at SMK TI Udayana. That is because the characteristics of mathematics and ICT different from other subjects. Math and ICT are more likely to sample questions that require a lot of facilities quiz, while the other subjects may be a lot of explaining concepts, thus requiring more space to display material.

Based on these problems, then made a decision support system to be able to choose a blended learning platforms that is suitable for the Mathematics and ICT learning at SMK TI Udayana.

II. LITERATURE REVIEW

A. Decision Support System

In [1], Decision Support System is an interactive computer-based system that helps decision makers to utilize data and models to solve unstructured problems.

In [2], Decision Support System is an interactive, flexible, and adaptable computer-based information system, especially developed for supporting the solution of a non-structured management problem for improved decision making.

In [3], Decision Support System is a computer-based system that aids the process of decision making.

In [4], Decision support systems can aid human cognitive deficiencies by integrating various sources of information, providing intelligent access to relevant knowledge, and aiding the process of structuring decisions.

Based on some views above, a synthesis can be generally made that decision support systems is computer-based system used to solve unstructured problems based on specific criteria and integrated with a variety of resources so as to produce the optimal decision.

B. Blended Learning

In [5], Blended learning is a student-centered approach to creating a learning experience whereby the learner interacts with other students, with the instructor, and with content through thoughtful integration of online and face-to-face environments.

In [6], Blended learning is a strategic and systematic approach to combining times and modes of learning, integrating the best aspects of face-to-face and online interactions for each discipline, using appropriate ICTs.

In [7], Definitions of blended learning range from the very broad where practically any learning experience that integrates some use of ICTs qualifies, to others that focus on specific percentages of online curriculum and face to face instruction. Most people agree that blended learning combines teaching and learning methods from face to face, mobile and online learning and that it includes elements of both synchronous and asynchronous online learning options.

In [8], blended learning is a formal education program in which a student learns: (1) at least in part through online learning, with some element of student control over time, place, path, and/or pace; (2) at least in part in a supervised brick-and-mortar location away from home; (3) and the modalities along each student's learning path within a course or subject are connected to provide an integrated learning experience.

In [9], blended learning is the interdependent combination of face-to-face and online education. It involves combining the better of these two modes of learning in such a way that they complement and supplement each other. Effective blended learning occurs when online and face-to-face modalities are used to their full advantage for optimal interaction and when there is capacity for student-paced and student-directed learning.

In [10], blended Learning has been defined in a variety of ways in the current specialized literature. The most common and current definition states that blended learning combine face-to-face instruction with distance education delivery systems.

Based on some views above, a synthesis can be generally made that Blended Learning is a student-centered learning using a systematic approach that combines face-to-face learning and online learning aided by ICTs.

C. Weighted Product

In [11], one way of partially avoiding the influence of the normalization procedure on the final result is to use the weighted product method, whose principle is close to that of the weighted sum. Values are multiplied instead of added, and each alternative being evaluated as follows:

$$P_{(a_i)}=(a_{i1}^{w_1})*(a_{i2}^{w_2})*\ldots..*(a_{in}^{w_n})=\pi_j(a_{ij}^{w_j}) \quad \ldots\ldots\ldots\ldots(1)$$

In [12], Weighted Product Method use multiplication to connect the attribute ratings, where the ratings of each attribute must be raised first with the relevant attribute weights. This process is similar to the process of normalization. Preferences for alternative A_i is given as follows:

$$S_i = \prod_{j=1}^{n} x_{ij}^{w_j} \quad \text{with i = 1,2, ..., n and } w_j = 1 \ldots\ldots\ldots(2)$$

w_j is the power of positive value to attribute profits, and is negative for the cost attribute. Relative preference of each alternative, given as:

$$V_i = \frac{\prod_{j=1}^{n} x_{ij}^{w_j}}{\prod_{j=1}^{n} (x_{j^*})^{w_j}} \quad \text{with i = 1, 2, ..., n} \ldots\ldots\ldots\ldots(3)$$

V : Preferences alternatives considered as a vector V
x : Value of Criteria
w : Weight of Criteria / Sub-criteria
i : Alternative
j : Criteria
n : number of criteria

III. Methodology

A. Object and locations of the study

1) The object of the study was platforms of blended learning.

2) The locations were SMK TI Udayana in Mengwi, Bali.

B. Subject of the Study

The subjects of the study were 10 teachers in SMK TI Udayana.

C. Type of Data

The data in this study were quantitative data.

D. Technique of data collection

The data were collected through observation and questionnaire.

E. Technique of Data Analysis

The data of the study were analyzed descriptively.

IV. Result and Discussion

A. Result

1) Blended Learning Platform

Some choice for blended learning platform that can be used in the process of mathematics and ICT learning at SMK TI Udayana, among others:

a) Edmodo

In [13], Edmodo is a global education network that helps connect all learners with the people and resources needed to reach their full potential. Edmodo can be seen at https://www.edmodo.com/

Fig. 1. Edmodo Platform

b) Quipper School

In [14], Quipper School is a FREE online platform for teachers and students. Quipper School consists of two parts: *LINK for teachers*, and *LEARN for students*. Quipper School

Link is where teachers manage their classes online and check students' progress. Quipper School Learn is where students study. It's packed with features that make learning safe and fun. Quipper School can be seen at https://school.quipper.com/en-PH/

Fig. 2. Quipper School Platform

c) Moodle

In [15], Moodle is a learning platform designed to provide educators, administrators and learners with a single robust, secure and integrated system to create personalized learning environments. Moodle can be seen at https://moodle.org/

Fig. 3. Moodle Platform

d) Kelase

In [16], Indonesia's online education space just got another boost of confidence today as ***Kelase***, a private social network for education, received an undisclosed amount seed funding from PT Insights Investments, a financial and investment firm in Indonesia. The money will be used for Kelase's product development, recruitment, and system maintenance. Kelase rolled out its trial version on June 2014. The startup allows education institutions to have their own social networks. Teachers and students can store and share numerous files on Kelase including education videos, e-books, and academic calendars some of which Kelase itself provides. Kelase can be seen at http://www.kelase.com/

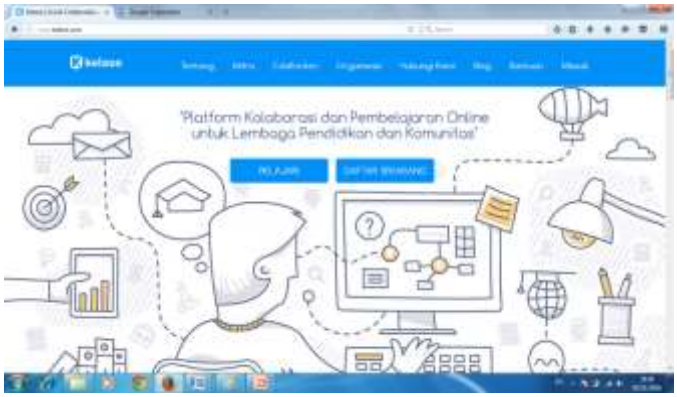

Fig. 4. Kelase Platform

2) Results of selection the Blended Learning Platform through calculation Weighted Product Method

Results of selection the Blended Learning Platform for Mathematics and ICT learning at SMK TI Udayana through calculation Weighted Product methods can be seen in Table I below.

TABLE I. RESULTS OF SELECTION THE BLENDED LEARNING PLATFORM FOR MATHEMATICS AND ICT LEARNING AT SMK TI UDAYANA

Platforms	Criterion			
	C1	C2	C3	C4
Edmodo	84	85	86	84
Quipper School	85	86	80	84
Moodle	82	81	86	85
Kelase	85	84	83	84

Note:
C1: easy to used
C2: attractive display
C3: large data capacity
C4: completed facilities

The weight for making a decision for each criterion is as follows.

C1: 5
C2 :4
C3: 4
C4: 4

The complete weighted product calculation to obtain the decision result can be explained as follows.

First a correction of weight is done such as $\sum w = 1$. Thus, it is obtained that $w_1 = 0.2941$; $w_2 = 0.2353$; $w_3 = 0.2353$; and $w_4 = 0.2353$.

Category of each criteria:

- Criterion C_1 is an advantage criterion.
- Criterion C_2 is an advantage criterion.
- Criterion C_3 is an advantage criterion.
- Criterion C_4 is an advantage criterion.

Then vector S can be calculated as folows:

$$S_1 = (84^{0.2941})(85^{0.2353})(86^{0.2353})(84^{0.2353}) = 84.702$$

$$S_2 = (85^{0.2941})(86^{0.2353})(80^{0.2353})(84^{0.2353}) = 83.793$$

$$S_3 = (82^{0.2941})(81^{0.2353})(86^{0.2353})(85^{0.2353}) = 83.387$$

$$S_4 = (85^{0.2941})(84^{0.2353})(83^{0.2353})(84^{0.2353}) = 84.056$$

The value of vector V to be used for ranking can be calculated as follows.

$$V_1 = \frac{84.702}{84.702+83.793+83.387+84.056} = 0.252$$

$$V_2 = \frac{83.793}{84.702+83.793+83.387+84.056} = 0.249$$

$$V_3 = \frac{83.617}{84.702+83.793+83.387+84.056} = 0.248$$

$$V_4 = \frac{84.056}{84.702+83.793+83.387+84.056} = 0.250$$

Based on the calculation of the vector V obtained the greatest value that is at V_1 by 0.252. The visualization of calculation can also be demonstrated by the following application program.

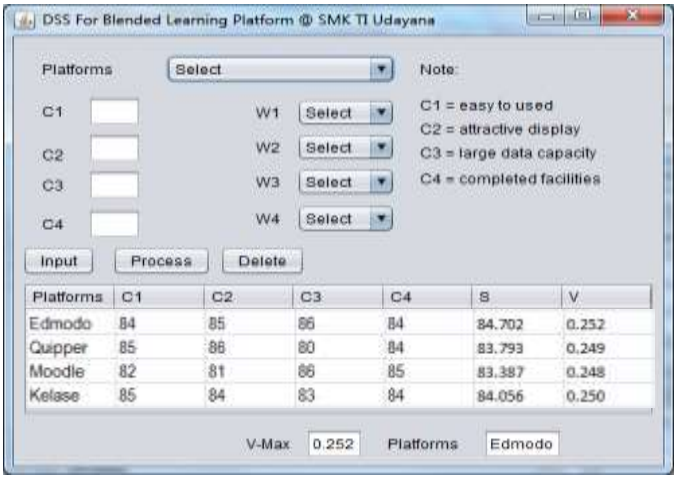

Fig. 5. DSS For Blended Learning Platform at SMK TI Udayana

B. Discussion

Based on the results of the study there were four blended learning platform that is offered for use in the process of mathematics and ICT learning at SMK TI Udayana, among others: Edmodo, Quipper School, Moodle and Kelase.

Calculation of the weighted product method based on inputted values into the four criteria. The calculations show the results of the largest-value vector V = 0.252, located at V_1, so Edmodo chosen as the blended learning platforms in mathematics and ICT learning at SMK TI Udayana.

Development of decision support system to selection the blended learning platforms for Mathematics and ICT Learning at SMK TI Udayana visualized using the Java programming language and MySQL database.

V. CONCLUSIONS

Based on the results of research and discussion, we can conclude that the blended learning platforms that is selected to facilitate the learning process of Mathematics and ICT at SMK TI Udayana is Edmodo, because it is based on the calculation of Weighted Product got the highest achievement when compared to other platforms.

REFERENCES

[1] R.H. Sprague, and E.D. Carlson, Building Effective Decision Support Systems. Englewood Clifts, N.J.: Prentice-Hall, Inc., 1982.

[2] P.N. Finlay, Introducing Decision Support Systems. Oxford, UK Cambridge, Mass., NCC Blackwell; Blackwell Publishers, 1994.

[3] E. Turban. 1995. Decision Support and Expert Systems: Management Support Systems. Englewood Cliffs, N.J.: Prentice Hall, 1995.

[4] M.J. Druzdzel, and R. R. Flynn, Decision Support Systems. Pittsburgh, Pennsylvania, U.S.A.: Taylor & Francis, 2010.

[5] R. Garrison and H. Kanuka, "Blended Learning: Uncovering its Transformative Potential in Higher Education," *Internet and Higher Education* 7, 2004, pp. 95–105.

[6] G. Saliba, L. Rankine, and H. Cortez, Fundamentals of Blended Learning. Sydney: University of Western Sydney, 2013.

[7] Department of Education and Early Childhood Development. Blended Learning: A Synthesis of Research Findings in Victorian Education 2006-2011. Melbourne: NEALS, 2012.

[8] http://www.christenseninstitute.org/blended-learning-definitions-and-models/

[9] https://bond.edu.au/about-bond/academia/learning-teaching/blended-learning

[10] R. T. Osguthorpe, and C. R. Graham, C.R, "Blended learning environments: Definitions and directions," The Quarterly Review of Distance Education, Vol. 4, No. 3, 2003, pp. 227-233.

[11] J. C. Pomerol, and S.B. Romero, Multicriterion Decision in Management: Principles and Practice. New York: Kluwer Academic Publishers, 2000.

[12] D.G. Hendra Divayana, "Development of Duck Diseases Expert System with Applying Alliance Method at Bali Provincial Livestock Office," International Journal of Advanced Computer Science and Applications, Vol. 5, No. 8, 2014, pp. 48-54.

[13] https://www.edmodo.com/about

[14] https://help.quipper.com/en/article_groups/access-codes/articles/what-is-quipper-school

[15] https://docs.moodle.org/31/en/About_Moodle

[16] https://www.techinasia.com/kelase-indonesia-seed-funding-education-social-network

Neural Backpropagation System for the Study of Obesity in Childhood

A. Medina-Santiago
Dept. Center of Investigation, Development and Innovation Technology (Cidit)
University of Science and Technology Descartes
Tuxtla Gutierrez, Chiapas, Mexico

L. C. Campos-Reyes
Nutrition Faculty
University of Veracruz
Veracruz, Mexico

E. M. Melgar-Paniagua
School Science Biology
Institute Polytechnic National
Mexico City, Mexico

A. Cisneros-Gómez, N. R. García-Chong
Dept. Center of Investigation, Development and Innovation Technology (Cidit), University Autonomy of Chiapas,
Faculty Medicine
University of Science and Technology Descartes
Tuxtla Gutierrez, Chiapas, Mexico

***Abstract*—This paper presents the development of a nutritional system using Backpropagation neural network, that is able to provide a clear and simple prediction problems of obesity in children up to twelve years, based on your eating habits during the day. For the development of this project has taken into account various factors, which are vital for the proper development of infants. A prediction system can offer a solution to several factors, which are not easily determined by convectional means.**

Keywords—prediction system; Nutrition; Backpropagation Neural Network; Obesity

I. INTRODUCTION

The ENSANUT 2006 warning about the risk in which there are more than 4 million children enter between 5 to 11 years, as the combined prevalence of overweight and obesity occurs in one out of four children [6, 7], also revealing that on weight and obesity has continued to increase in all ages, regions and socioeconomic groups, which has led our country to take first place in the world in obesity.

In Mexico, based on information from two national sources, it was find one built in 1999 and another one in 2006, it is known that the combined prevalence of overweight and obesity has increased across the population, but particularly in the school-age population. During this period, obsesity in children increased 33% and 53% children [7].

The adverse effect and risks to health obesity early in life include both short-term physical and psychosocial problems.

Longitudinal studies that childhood obesity suggest, after 3 years of age, long-term is associated with an increased risk of obesity in adulthood and with increased morbidity, persistence of associated metabolic disorders [6].

School age and adolescence are a crucial configuration steps eating habits and other lifestyles that persist in later, with repercussions not only at this stages as to the possible impact as a risk factor, but aslo in the even in adulthood and old age.

Although there is little information regarding eating habits at school age, there are reports that report that between 7-34% of children do not eat breakfast at home before going to school [7].

Except in some private schools, public are not places where you can buy food or have spaces where they can taste. However, playtime can buy food that sells school cooperative. This name is known to the members organizations of teachers and students, staff or parents, as allowed by the regulations in force, whose role is that student's appended process of production and consumption. These cooperative are not new amd the first regulation dates from 1934, the following was issued in 1937, in 1962 appears a new, updated in 1982, which is theoretically valid. It should be mentioned that the purpose of the cooperatives are esentialy related to educational and learning teamwork, assimilation processes of production and consumption, the possibility that the products are sold at a lower price that prevails in the promotes the marked and that earnings will be used to improve the school.

Nutrition is a vital issue, as vital body processes require the supply of materials and energy to provide the necessary elements for increase and repair of body tissues [8].

One should be aware that food is one of the pillars on which health is based. For better or worse, food is the mainstay of the formation and prevention of future disease and could be atherosclerosis, hypertension, mainly diabetic and different degress of obesity that plague our society. Therefore, we must start from small, balanced meals, so our body will be healthy at the same time avoiding any childhood diseases [11, 12].

There are an important aspect to consider about the power system is that this can not be generalized since each individual has different nutritional needs, that is why the alimentation depend on the activities performed by an individual throughout the day, i.e., it has to be directly proportional to their activities pied otherwise fall into malnutrition.

In nowadays society, the objectives of the child alimentation have expanded and now not only aims to achieve optimal growth and prevent malnutrition and disease occurrence caracals, but also, through the same, optimizer maturational development, establish healthy habits to prevent the onset of nutritional base diseases affecting adults, trying to get better quality of life and longevity.

As will be seen later, to secure as soon raised, we will use the Backpropagation neural network [1-4] that has some differences from traditional logic as it defines the training and classification of data, if the theory of neural networks to predict as a data set to obtain a desired output approach, particularly the prediction data.

The structure of the article is in section 2 history of the work of research, mathematical basis, neuronal structure. In stage 3 the results of the simulations of the neural system for the study of obesity with the defined variables. Section 4 is the discussion of the system compared to conventional system; Finally, section 5 shows the conclusions of the research.

II. Data Collection (Background)

A. Problem Statement

In Mexico, the overweigth and obesity is a serious public health affecting school children because of all socioeconomic classes.

He believies that schools primaries National System of Educatio, which have registered more than 95% of school-age children, are a plataform that can help reverse the serious problem of overweight if it is recognized that, for now, the school is closer to being an genetic obesity environment healthy, and that part of its mission is to promote, in various educational activities, the acquisition of styles of healthy eating and physical activity. While the building has to be animed primarily at children, aslo has to involve all social actors of change factors, such as parents, family, educational institutions, community authorities and, in particular, industry producing food and beverage processing, and by advertising industry print and online [14].

B. Justification

This research grew out of the need to consider one of the possible factors that cause overweight and obesity in children, and the relationship of these with the consumptionof foods that are sold within the shool cooperatives, hygiene, food handly, prepare hygienic measures, proper sanitation requirements and frequency of food consumption.

C. Hypothesis

The cooperative school meets the hygenic-Nutrient, where the food consumed within the school are a determining factor in the nutritional status of children, and applying neural network techniques can predict the behavior of infant obesity [9, 10, 13, 15].

D. Theoretical framework

We assesed the nutrional status of students using the criteria of the Official Mexican Standard NOM-008-SSA2-1993, Control Nutrition, Growth and Development of Children and Adolescents and evaluation form containing: Name, Grade and Group age, weigth, height, Hips (centimeters) Waist (centimeters), BMI and food intaje [6, 7].

We evaluated the school cooperative consider through a direct observation assessment tool designed to evaluate the conditions of this, both hygenically and nutritionally about te products that are sold at recess.

Also we identified the relationship between the consumption of foods that is sold in the Cooperative School with nutritional status of students, as it is a very impactor factor for the primary students. Finally, we developed a numerical prediction system with neural network artificial Backpropagation for prediction and reinforcement of the theoretical data acquired on the job, obtained comparative test with the results of observations made, based on a sheet of data and theory a biological neuron [13, 15], and subsequently implement the system of artificial neural network with Bakcpropagation learning algorithms characterized by the equation [1, 2]:

$$a^4 = f^4(w^4 f^3(w^3 f^2(w^2 f^1(w^1 p+b^1)+b^2)+b^3)+b^4) \quad (1)$$

E. Neural network [1-4]

Neural nerwork consist of a simulation of the observed properties of the biological diversity of neural systems throgh mathematical models recreated through artificial mechanisms (an integrated circuit or a computer). The aim is to ensure that the mechanies give similar answer to which are able to give to the brain.

A neural network consists of units called neurons, and each neuron receives a set of inputs through interconnections and makes an exit. This output is given by three functions:

- A propagation function, which generally consists of the sum of each input multiplied by but their interconnection. If we weight is positive, the connection is called excitatory, if negative, is called inhibitor.
- An activation function that modifies the former can not exist, being here the diffusion of the same function.
- A transfer function, which applies to the value returned by the ouput function of the neuron and generally is given by the understanding that we can give to the outputs.

F. Structure

Most scientist agree that an artificial neural network ANN [3] is very different in terms of structure of an animal brain. As brain, an ANN consist of a set of simple units massively parallel processing and connections between these units where the network intelligence.

Biologically the brain learns through the reorganization of synaptic connections between individual neurons. Similarly, RNA having a large number of virtual processors inteconnected in a simplified manner to simulate the functionality of biological neurons Figure 1. In this simulation [4], the mechanism reorganization synaptic connections biological models with weights that are adjusted during the learning phase. An ANN trained, the weights determined set of knowledge of RNA and is capable of solving a problem.

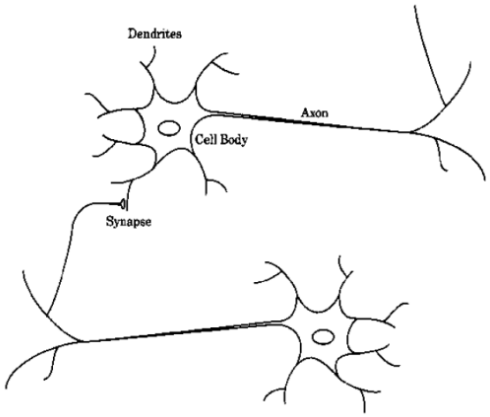

Fig. 1. A schematic drawing of biological neurons

Furthermore, each neuron is associated with a mathematical functions called transfer function. This function generatest the sugnal output from the neuron input signals. The entry of the function is the sum of all input signals but by the connection associated with that signal (Figure 2).

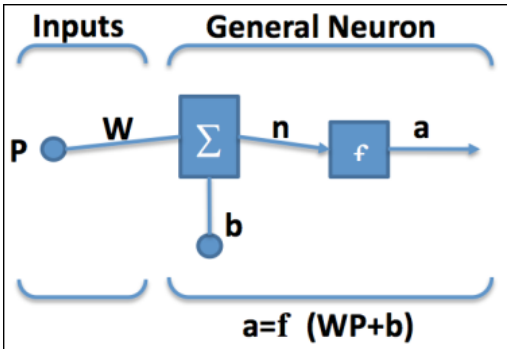

Fig. 2. Entrace of a single neuron

G. The multilayer perceptron [1-4]

It basically consists of a layer of neurons with weights and adjustable threshold; this neural system may be called a neural network because the connections exist in its entirety the Perceptron training is to determine the adjustment to be performed each neuron weight to the output error is zero.

Backpropagation algorithm is a generalization of the LMS algorithm; both algorithms perform its task of updating weights and profits based on the means square error. The network works under supervised learning and therefore requires an array of workout that will describe each output and expected output value. The structure Backpropagation neural network was shown in Figure 3.

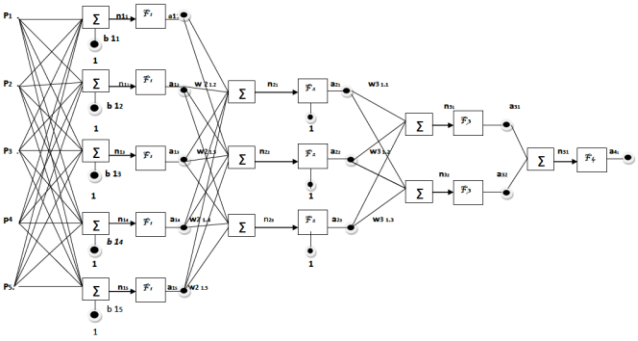

Fig. 3. Architecture Multilayer Perceptron with Backpropagation Algorithm

III. RESULTS

Data from the savanah of data (Table 1) should be reads as described promptly: results output with a neural network [10, 13, 15] on equal 1.9119 and 0.9326 for girl children; regarding this outcome data savannah Girls has a degree 3 of obesity and the child would have an obesity grade 2; dependent on the age, BMI, ICC and food intake [11, 12, 13].

TABLE I. DATA FROM THE SAVANNAH OF DATA

Ages children	**Prediction**		
	Girl	***Boy***	***Observations***
6	1.8056[a]	0.8640	Obese / moderately obese
7	0.1258	0.8645	Not Obese / moderately obese
8	0.8229	0.8647	Moderately obese / moderately obese
9	0.5027	0.8641	Not Obese / moderately obese
10	2.2126	0.8641	Obese / moderately obese
11	1.7740	0.8641	Obese / moderately obese

[a] Data Savannah of data obtained in the field.

The following figures show numerical results of the prediction system used.

Test performed for behaviour in Women
Test = [age, IMC, ICC, Food Intake]
Test 1 = [1;1;3;3]; target = sim (net, test 1)
Output = 1.2354
Test 2 = [12;2;2;3]; target = sim (net, test 2)
Output = 0.8142
Test 3 = [12;1;1;3]; target = sim (net, test 3)
Output = 0.3132
Test 4 = [2;1;3;2]; target = sim (net, test 4)
Output = 0.5377
Test 5 = [8;2;2;3]; target = sim (net, test 5)
Output = 0.7908

Fig. 4. Prediction for women with different age, BMI, WHR and food intake

Test performed for behaviour in Men
Test = [age, IMC, ICC, Food Intake]
Test 1 = [6;1;2;3]; target = sim (net, test 1)
Output = 0.8665 Not Obese
Test 2 = [5;1;2;3]; target = sim (net, test 2)
Output = 0.8266 Not Obese
Test 3 = [6;2;2;2]; target = sim (net, test 3)
Output = 0.8942 Moderately Obese

Fig. 5. Prediction for men with different age, BMI, WHR and food intake

Test performed for behaviour in Men
Test = [age, IMC, ICC, Food Intake]
Test 1 = [1;1;3;3]; target = sim (net, test 1)
Output = 0.9610
Test 2 = [12;2;2;3]; target = sim (net, test 2)
Output = 0.5037
Test 3 = [2;1;3;2]; target = sim (net, test 3)
Output = 0.9505
Test 4 = [8;2;2;3]; target = sim (net, test 4)
Output = 0.5489

Fig. 6. Prediction for men with different age, BMI, WHR and food intake

The following figures shows the neural behavior prediction system.

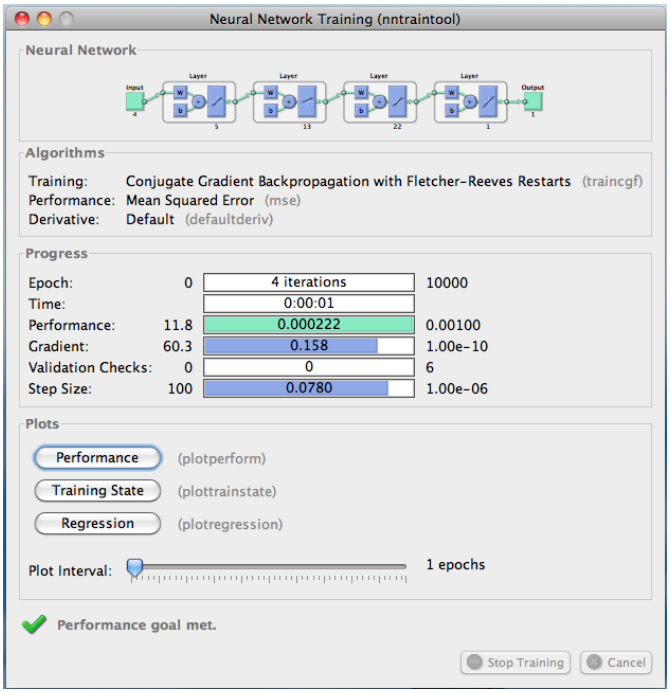

Fig. 7. Training of the ANN-BP

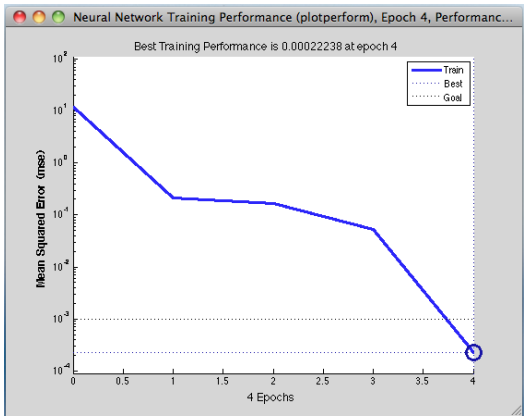

Fig. 8. Performance of the RNA-BP in sampling error

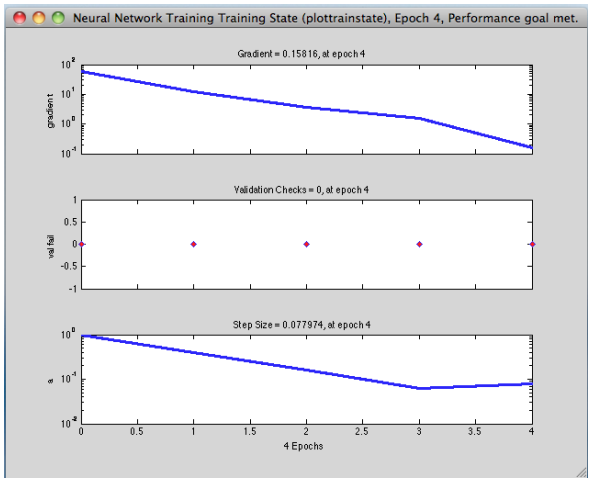

Fig. 9. State of training of the ANN-BP characterizing the system output

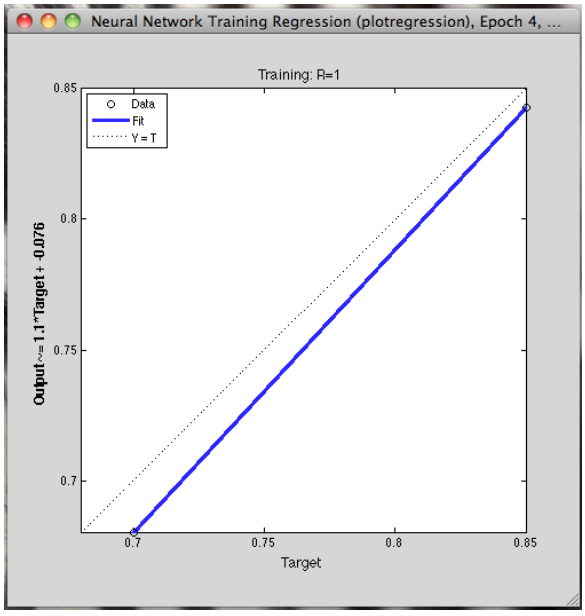

Fig. 10. Trainging Regression-BP RNA

```
%SISTEMA DE NUTRICION
%MTRA. LITA CAMPOS
%DR. MEDINA
%UNIVERSITY VERACRUZ
%School of Nutrition
%Institute Techonolog of Tuxtla Gutierrez
%Posgrade Biochemical and Mechatronic

%P=[EDAD DEL NIÑO,IMC,ICC,INGESTA DE ALIMENTOS]
P=[6 11;1 3;1 3;1 3];
%T=[0.70 0.85;0.78 0.94];
T=[0.70 0.85];
net1=newff(minmax(P),[5,13,22,1],{'tansig','logsig','tansig','purelin'},'traincgf');
net1.trainParam.show=5;
net1.trainParam.lr=.5;
net1.trainParam.epochs=10000;
net1.trainParam.goal=1e-3;
[net1,tr]=train(net1,P,T);
NINA=sim(net1,P)
error=T-NINA
```

Fig. 11. Pseudocode predictive system RNA-BP development

IV. Discussion

Them results obtained with the network neuronal are of great contribution whereas a comparison of the exercise of the nutritionist without it tool and with the use of the tool increase is effectiveness, decreased the time of diagnostic of them data, reduction in the time of search in the table of nutrition to diagnose the obesity of the child school. This tool can be purchased with a system expert working group currently developing and shall submit to the test in 3 months.

V. Conclusions

The findings of the predictive system based on Backpropagation neural network is an effectiveness of about 99.99% of the comparative data, generating predictions on the prospects of effective school nutrition, dependent variables mentioned above characteristic. Authors and Affiliations

Acknowledgment

We thank the university of veracruz, faculty of nutrition for the contributions in the data sheets of children at primary level for the field tests; With a sample of 20 public schools and 10 private schools. We thank the teachers, doctors and students for their support.

References

[1] Martin T. Hagan, Howard B. Denuth, Mark Beale, Orlando de Jesus, Neural Networks Design, 2nd Edition, Pws Pub Co; Edición: Har/Dskt (1 de diciembre de 2014.

[2] Ryszard Tadeusiewicz and Rituparna Chaki, Exploring Neural Networks with C#, CRC Press, 2014.

[3] Scientific Books, Decision Trees, Regression and Neural Network Models with Data Minning Tools, Amazon Digital. 2015.

[4] Aurelio Uncini, Fundamentals of Adaptive Signal Processing (Signals and Communication Technology), Springer. 2015.

[5] Obesity Implications and comprehensive management. Childhood obesity. Xenical. 2013.

[6] Public health n2 V47 Mexico. Cuernavaca March / April 2005. Impact escolares a breakfast program in the prevalence of obesity and risk factors for obesity in children Sonora.

[7] Olaiz-Fernández G, Rivera-Dommarco J, Shamah-Levy T, Rojas R, Villalpando-Hernández S, Herández-Avila M, Sepúlveda-Amor J. National Health Survey and Nutricion 2006. Cuernavaca, Mexico: National Public Health Institute 2006.

[8] R Monteiro R, Azevedo I. Chronic inflammation in obesity and the metabolic syndrome. Mediators Inflamm 2010.

[9] Hung-Teng Chang, Pin-Chang Chen, Han-Chen Huang, De-Hua Lin, A Study on the Application of Neural Network to the Prediction of Weight Control, International Journal of Engineering Research and Development. Volume 5, Issue 11 (February 2013), PP. 78-85.

[10] Yu-Chuan Chang, Pei-Hsin Lin, Chun-Chang Chen, Ren-Guey Lee, Jing-Siang Huang, Tsai-Hsuan Tsai, eFurniture for home-based frailty detection using artificial neural networks and wireless sensors, Medical Engineering & Physics, February 2013Volume 35, Issue 2, Pages 263–268.

[11] Blaum, C.S., Xue, Q.L., Michelon, E., Semba, R.D., Fried, L.P. The association between obesity and the frailty syndrome in older women: the women's health and aging studies. Journal of the American Geriatrics Society. 2005; 53:927–934.

[12] Raman Paranjape, Asha Sadanand, Multi-Agent systems for Healthcare Simulation and Modeling: Applications for System Improvement, 1st Edition, Medical Information Science Reference. 2013.

[13] Ashley N. Gearhardt, Sonja Yokum, Eric Stice, Jennifer L. Harris and Kelly D. Brownell, Relation of obesity to neural activation in response to food commercials, Soc Cogn Affect Neurosci (2014) 9 (7): 932-938.

[14] J Liang, B E Matheson, W H Kaye and K N Boutelle, Neurocognitive correlates of obesity and obesity-related behaviors in children and adolescents, International Journal of Obesity (2014) 38, 494–506.

[15] Seyed Taghi HeydariSeyed Mohammad Taghi Ayatollahi, Najaf Zare, Comparison of Artificial Neural Networks with Logistic Regression for Detection of Obesity, Journal of Medical Systems, August 2012, Volume 36, Issue 4, pp 2449–2454.